Available online at www.sciencedirect.com
SCIENCE DIRECT®
Journal of Computational Physics 188 (2003) 399–433
JOURNAL OF COMPUTATIONAL PHYSICS
www.elsevier.com/locate/jcp

Stability of perfectly matched layers, group velocities and anisotropic waves

E. Bécache [a], S. Fauqueux [a,b,*], P. Joly [a]

[a] *INRIA, Domaine de Voluceau-Rocquencourt, BP 105, F-78153 Le Chesnay Cédex, France*
[b] *IFP, 1 avenue Bois Préau, 92500 Reuil Malmaison, France*

Received 15 November 2001; received in revised form 17 February 2003; accepted 22 February 2003

Abstract

Perfectly matched layers (PML) are a recent technique for simulating the absorption of waves in open domains. They have been introduced for electromagnetic waves and extended, since then, to other models of wave propagation, including waves in elastic anisotropic media. In this last case, some numerical experiments have shown that the PMLs are not always stable. In this paper, we investigate this question from a theoretical point of view. In the first part, we derive a necessary condition for the stability of the PML model for a general hyperbolic system. This condition can be interpreted in terms of geometrical properties of the slowness diagrams and used for explaining instabilities observed with elastic waves but also with other propagation models (anisotropic Maxwell's equations, linearized Euler equations). In the second part, we specialize our analysis to orthotropic elastic waves and obtain separately a necessary stability condition and a sufficient stability condition that can be expressed in terms of inequalities on the elasticity coefficients of the model.

Keywords: Perfectly matched layers; Absorbing layers; Elastodynamics; Stability; Hyperbolic systems; Fourier analysis; Linearized Euler equations; Anisotropy

1. Introduction

Perfectly matched layers (PML) is a recent technique for simulating the absorption of waves in open domains, which provides a very efficient alternative to the use of absorbing boundary conditions in many applications. The idea is to surround the computational domain with an absorbing layer (the PML region) so that the coupled system possesses the property of generating no reflection at the interface between the free medium and the artificial absorbing medium. This technique has been initially introduced by Bérenger [10] for Maxwell's equations, and has been widely used for the simulation of time dependent electromagnetic

* Corresponding author.
E-mail addresses: Eliane.Becache@inria.fr (E. Bécache), Sandrine.Fauqueux@inria.fr (S. Fauqueux), Patrick.Joly@inria.fr (P. Joly).

0021-9991/03/$ - see front matter
doi:10.1016/S0021-9991(03)00184-0

waves as well as Helmholtz-like equations (e.g. [11,12,28,37,39]). The method has been extended to various propagation models (the paraxial wave equations [15], the linearized Euler equations [22,24,32], etc.), including in particular elastic wave propagation in isotropic [21] and anisotropic media [17]. Trying to use these PMLs for computing the propagation of seismic waves, we observed exponential blow up phenomena in some numerical experiments involving anisotropic media. Analogous exponential instabilities have been also observed in the simulation of non-destructive testing experiments [19]. This has motivated us to look at the question of the *well-posedness* and the stronger notion of *stability* of PMLs, introduced in [6], for anisotropic elastic waves. It is important here to make precise the distinction (see Section 3) between these two notions (see also [33] for similar considerations): by well-posedness, we mean that there exists a unique solution and that the L^2 norm of the solution can be bounded by some norm of the initial conditions multiplied by a constant $C(t)$. This does not prevent the solution from blowing up exponentially in time: in this case, we shall say that the problem is unstable. As a matter of fact, if, from the mathematical point of view, the difference between an ill-posed problem and an unstable (but well-posed) problem is fundamental, for practical applications, it is not, since it is difficult to distinguish these two cases numerically. A more pertinent concept is the one of stability, which imposes an estimate of the type $C(t) \leqslant Ct^k$. In particular, this concept of stability does not exclude a linear growth as the one studied in [2,4] for Maxwell's equations. Furthermore, note that the notion of stability described here is linked to the continuous model and is distinct from the numerical stability related to a particular numerical scheme. For an unstable model, no particular discretization prevents the solution from blowing up exponentially.

This type of mathematical questions has already been widely investigated by several authors [6,27,29,30,38] in the case of Maxwell's equations. For elastodynamics equations, it is easy to show that the PML model is well-posed (cf. Section 3.2) but we will show that it can be unstable for some anisotropic media. The outline of this paper is as follows.

- In Section 2, we recall the propagation equations for elastic waves in a 2D orthotropic medium (Section 2.1) and recall the important notion of slowness diagrams (Section 2.2). In Section 2.3, we present the construction of the standard PML model for a general first order hyperbolic system and specialize it to elastic waves in Section 2.4. Finally Section 2.5 is devoted to various simulations that point out the instability phenomena that motivate the present works.
- In Section 3 we derive a necessary condition for the stability of the PML model for a general hyperbolic system (Theorem 2). This condition can be interpreted in terms of group velocities and phase velocities (also related to geometrical properties of the slowness diagrams) and is more precisely related to the existence of so-called backward propagating waves. We can use this criterion for explaining instabilities observed with elastic waves but also with other propagation models (anisotropic Maxwell's equations, linearized Euler equations) and it seems to show that these instabilities can occur only (but not necessarily) with models involving anisotropy. Finally we present numerical simulations showing that this geometrical criterion is not sufficient for stability in the case of elastic waves.
- In Section 4, we specialize our analysis to orthotropic elastic waves and obtain separately a necessary stability condition (Theorem 4) and a sufficient stability condition that can be expressed in terms of inequalities on the elasticity coefficients of the model (Theorem 5).

2. Orthotropic elastic waves and PML model

2.1. The elastodynamics system

In this paper we work in two dimensions. All the indices i, j, k, l take their values in $\{1, 2\}$. $x = (x_1, x_2)$ denotes the space variable and ∂_i holds for the derivation with respect to x_i. Throughout this section, we

shall use the Einstein convention on repeated indices for summation. Let us introduce the equations of elastodynamics in a 2D homogeneous medium

$$\rho \frac{\partial^2 u}{\partial t^2} - \operatorname{div} \sigma(u) = 0, \tag{1}$$

where $u = (u_i)$ denotes the displacement field, $\rho > 0$ the density, $\sigma(u) = \sigma_{ij}(u)$ the stress tensor and

$$\operatorname{div} \sigma = \begin{pmatrix} \partial_1 \sigma_{11} + \partial_2 \sigma_{12} \\ \partial_1 \sigma_{12} + \partial_2 \sigma_{22} \end{pmatrix}.$$

The stress tensor is related to the strain tensor $\varepsilon(u)$ defined by

$$\varepsilon_{ij}(u) = \frac{1}{2}(\partial_i u_j + \partial_j u_i), \tag{2}$$

by Hooke's law

$$A\sigma = \varepsilon(u) \Longleftrightarrow \sigma = C\varepsilon(u) = A^{-1}\varepsilon(u). \tag{3}$$

The fourth-order tensor C of elasticity coefficients satisfies the classical symmetries [3]

$$C_{ijkl} = C_{klij} = C_{jikl}. \tag{4}$$

Moreover, it is positive definite

$$C_{ijkl}\xi_{ij}\xi_{kl} \geqslant \alpha \|\xi\|^2 = \alpha \xi_{ij}\xi_{ij} \tag{5}$$

for all symmetric tensor ξ.

Notation. As it is classical, the symmetries (4) of the tensor C allows us to simplify its representation into a 3×3 matrix c_{pq}, still denoted by C for simplicity, such that

$$C_{ijkl} = c_{p(i,j),p(k,l)},$$

where the function p is defined by

$$p(1,1) = 1, \quad p(2,2) = 2, \quad p(1,2) = p(2,1) = 3.$$

Orthotropic media. In an orthotropic medium whose principal axes coincides with the (x, y) axes, we have $c_{13} = c_{23} = 0$ so that [3]

$$C = \begin{pmatrix} c_{11} & c_{12} & 0 \\ c_{12} & c_{22} & 0 \\ 0 & 0 & c_{33} \end{pmatrix}.$$

With this notation, condition (5) becomes ($|\cdot|$ denotes the Euclidean norm in $\mathbb{R}^3$)

$$c_{11}V_1^2 + c_{22}V_2^2 + 2c_{12}V_1V_2 + c_{33}V_3^2 > \alpha|V|^2 \quad \forall V \in \mathbb{R}^3, \tag{6}$$

which is equivalent to the inequalities

$$c_{11} > 0, \quad c_{22} > 0, \quad c_{33} > 0, \quad c_{11}c_{22} - c_{12}^2 > 0. \tag{7}$$

For an isotropic medium, which is of course a particular orthotropic material, the coefficients can be expressed in terms of Lamé's coefficients $\lambda > 0$ and $\mu \geqslant 0$:

$$c_{11} = c_{22} = \lambda + 2\mu, \quad c_{12} = \lambda, \quad c_{33} = \mu. \tag{8}$$

In order to apply the general construction of the PML model, we will need to reformulate the propagation equations as a first-order system, the so-called velocity–stress formulation

$$\begin{aligned} &\rho \frac{\partial v}{\partial t} - \operatorname{div} \sigma = 0, \\ &A \frac{\partial \sigma}{\partial t} - \varepsilon(v) = 0, \end{aligned} \tag{9}$$

where $v = \partial_t u$ is the velocity field.

2.2. Harmonic plane waves and slowness diagrams

Plane waves are particular solutions of (1) on the form

$$u(x,t) = D e^{i(\omega t - k.x)}, \quad D \in \mathbb{R}^2, \ x = (x_1, x_2), \tag{10}$$

where $k \in \mathbb{R}^2$ is the wave vector, $\omega \in \mathbb{R}$ the circular frequency and D the displacement vector (or polarization vector). We also introduce

$$\begin{aligned} &K = \frac{k}{|k|}, \quad \text{the unit propagation direction,} \\ &\mathscr{V} = \frac{\omega}{|k|}, \quad \text{the phase velocity,} \\ &\vec{S} = \frac{k}{\omega}, \quad \text{the slowness vector.} \end{aligned} \tag{11}$$

Plane waves of the form (10) are solutions of (1) if the circular frequency and the wave vector k satisfy a relation, called *dispersion relation*. In order to write this relation, it is useful to introduce Chrystoffel's tensor [3]

$$\Gamma_{ij}(k) = C_{iljm} k_l k_m, \tag{12}$$

which can be rewritten with the new notation

$$\Gamma(k) = \begin{pmatrix} c_{11}k_1^2 + 2c_{13}k_1k_2 + c_{33}k_2^2 & c_{13}k_1^2 + (c_{12}+c_{33})k_1k_2 + c_{32}k_2^2 \\ c_{13}k_1^2 + (c_{12}+c_{33})k_1k_2 + c_{32}k_2^2 & c_{33}k_1^2 + 2c_{23}k_1k_2 + c_{22}k_2^2 \end{pmatrix}.$$

So, in an orthotropic medium, we have

$$\Gamma(k) = \begin{pmatrix} c_{11}k_1^2 + c_{33}k_2^2 & (c_{12}+c_{33})k_1k_2 \\ (c_{12}+c_{33})k_1k_2 & c_{33}k_1^2 + c_{22}k_2^2 \end{pmatrix}. \tag{13}$$

We notice that $\Gamma(k)$ is homogeneous of degree 2 with respect to k:

$$\Gamma(\alpha k) = \alpha^2 \Gamma(k). \tag{14}$$

It is well known that, due to (5), for any $k \neq 0$, $\Gamma(k)$ is symmetric positive definite [3]. Substituting (10) into (1), one sees that the polarization vector D must be an eigenvector of $\Gamma(k)$ associated to the eigenvalue $\rho\omega^2$:

$$\Gamma(k)D(k) = \rho\omega^2 D(k) \Longleftrightarrow \Gamma(K)D = \rho \mathscr{V}^2 D.$$

The frequency ω and the wave vector k are thus related by the following *dispersion relation*:

$$F_2(\omega,k) \equiv \det(\Gamma(k) - \rho\omega^2 I) = 0, \tag{15}$$

where I is the identity matrix. Considering (15) as an equation in the frequency ω for a given value of the wave vector k, we obtain four solutions

$$\omega = \pm\omega_{\mathrm{QP}}(k), \quad \omega = \pm\omega_{\mathrm{QS}}(k), \quad (\omega_{\mathrm{QP}}(k) > 0,\ \omega_{\mathrm{QS}}(k) > 0),$$

where $\gamma_{\mathrm{QP}}(k) = \rho\omega_{\mathrm{QP}}^2(k) \geqslant \gamma_{\mathrm{QP}}(k) = \rho\omega_{\mathrm{QS}}^2(k)$ are the two positive eigenvalues of $\Gamma(k)$ associated to the respective eigenvectors $D_{\mathrm{QP}}(k)$ and $D_{\mathrm{QS}}(k)$,

- For $\omega = \pm\omega_{\mathrm{QP}}(k)$ and $D//D_{\mathrm{QP}}(k)$, the wave is called quasi-longitudinal.
- For $\omega = \pm\omega_{\mathrm{QS}}(k)$ and $D//D_{\mathrm{QS}}(k)$, the wave is called quasi-transverse.

The expressions of the eigenvalues are

$$\begin{aligned}
\gamma_{\mathrm{QP}}(k) &= \frac{1}{2}\left(\Gamma_{11}(k) + \Gamma_{22}(k) + \sqrt{(\Gamma_{11}(k) - \Gamma_{22}(k))^2 + 4\Gamma_{12}(k)^2}\right),\\
\gamma_{\mathrm{QS}}(k) &= \frac{1}{2}\left(\Gamma_{11}(k) + \Gamma_{22}(k) - \sqrt{(\Gamma_{11}(k) - \Gamma_{22}(k))^2 + 4\Gamma_{12}(k)^2}\right).
\end{aligned} \tag{16}$$

In particular in an isotropic medium, we recover the usual pressure and shear waves:

- $\omega_{\mathrm{QP}}(k) = |k|\mathscr{V}_P$, $\mathscr{V}_P = \sqrt{\frac{\lambda+2\mu}{\rho}}$ (in this case $D^{QP}(k)//k$),
- $\omega_{\mathrm{QS}}(k) = |k|\mathscr{V}_S$, $\mathscr{V}_S = \sqrt{\frac{\mu}{\rho}}$ (in this case $D^{QS}(k) \perp k$).

Slowness diagram and group velocity. By homogeneity, the dispersion relation (15) can be rewritten as

$$F_2\left(1, \frac{k}{\omega}\right) = F_2(1, \vec{S}) = 0. \tag{17}$$

By definition, the slowness diagram is the set of points, in the plane of slowness vectors $\vec{S} = k/\omega$, that satisfy (17). It is also the union of two curves whose equations in polar coordinates are

$$|\vec{S}| = \frac{1}{\omega_{\mathrm{QP}}(K)} \quad \text{and} \quad |\vec{S}| = \frac{1}{\omega_{\mathrm{QS}}(K)}.$$

We give in Fig. 1 two examples of slowness diagrams. On the left, for an isotropic medium (the two curves are two circles, respectively, of radius $1/\mathscr{V}_P$ and $1/\mathscr{V}_S \geqslant 1/\mathscr{V}_P$) and on the right for an anisotropic medium ($c_{11} = c_{22} = 20,\ c_{33} = 2,\ c_{12} = 3.8$).

For each branch of solution $k \to \omega(k)$ of the dispersion relation, one defines the *group velocity* as follows:

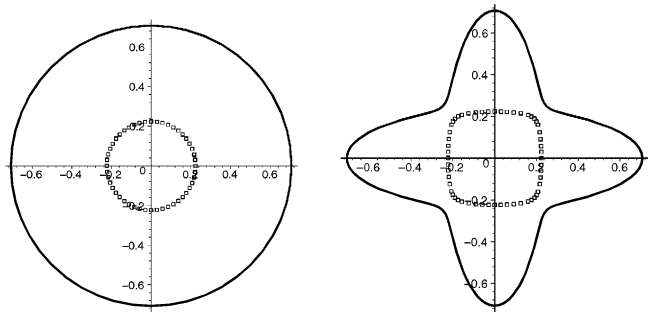

Fig. 1. Slowness diagrams. Left: isotropic medium. Right: orthotropic medium.

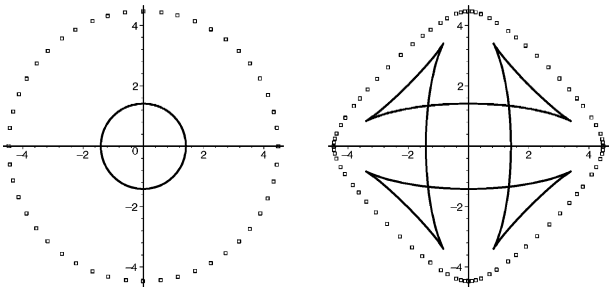

Fig. 2. Waves fronts. Left: isotropic medium. Right: orthotropic medium.

$$\vec{V}_{\mathrm{g}}(k) = \nabla_k \omega(k). \tag{18}$$

For almost every k, the two branches do not intersect (it can happen only if $c_{33} = c_{11}$ or $c_{33} = c_{22}$ and for at most four particular directions) and using (15), by implicit function theorem, it is easy to see that the group velocity can also be expressed as

$$\vec{V}_{\mathrm{g}}(k) = -\left(\frac{\partial F_2}{\partial \omega}(\omega(k),k)\right)^{-1} \nabla_k F_2(\omega(k),k) = -\left(\frac{\partial F_2}{\partial \omega}(1,\vec{S})\right)^{-1} \nabla_k F_2(1,\vec{S}), \tag{19}$$

which shows that the *group velocity is orthogonal to the slowness curves.* Finally, *the wave fronts* are defined as the curves described by the extremities of the group velocities. These curves permit to predict the localization of the energy of a solution emitted from a point source (see Fig. 2).

Remark 1. One can notice that the dispersion relation of the first-order system (9) is not identical to the second order's one F_2: it has the additional eigenvalue 0 and can be expressed as

$$F_1(\omega,k) = \omega^{\ell_0} F_2(\omega,k) \quad (\ell_0 = 1 \text{ in 2D and } \ell_0 = 3 \text{ in 3D}). \tag{20}$$

2.3. The PML model for a general first-order evolution problem

The principle of the perfectly matched layers has been first introduced by Bérenger [10], for electromagnetic waves and has been, since then, applied in numerous applications. In [17], the authors have shown that it is possible to write a systematic way of designing a PML model for a general first-order hyperbolic system. In this section we briefly describe this general construction. Consider a general first-order hyperbolic system, posed initially in $\mathbb{R}^m$, of the form

$$\partial_t u - A_1 \partial_1 u - A_2 \partial_2 u = 0, \tag{21}$$

where u is a m-vector, A_1 and A_2 are $m \times m$ matrices.

Let us briefly recall the definitions of hyperbolicity (see [26]). We set $\mathscr{A}(k) = k_1 A_1 + k_2 A_2$. System (21) is hyperbolic if, for all $k \in \mathbb{R}^2$, the eigenvalues of $\mathscr{A}(k)$ are real. It is strongly hyperbolic if furthermore, for all $k \in \mathbb{R}^2$, $\mathscr{A}(k)$ can be diagonalized (if not it is weakly hyperbolic). It is strictly hyperbolic if, for all $k \in \mathbb{R}^2$, the eigenvalues of $\mathscr{A}(k)$ are real and distinct.

The formal construction of a PML in the x_1 direction (parallel to the x_2 axis) consists in: (i) introducing a splitting of the field $u = u^1 + u^2$, such that the unknown u^1 is only "associated" to the derivatives with respect to x_1, and u^2 to the derivatives with respect to x_2, (ii) introducing an anisotropic damping factor only on the u^1 component. We then obtain the following PML system:

$$\begin{aligned} &\partial_t u^1 + \zeta(x_1)u^1 - A_1\partial_1(u^1+u^2) = 0,\\ &\partial_t u^2 - A_2\partial_2(u^1+u^2) = 0, \end{aligned} \tag{22}$$

where $\zeta(x_1) = 0$ for $x_1 < 0$ and $\zeta(x_1) \geqslant 0$ for $x_1 \geqslant 0$.

In the frequency domain, system (22) becomes

$$\begin{aligned} &\mathrm{i}\omega u^1 + \zeta(x_1)u^1 - A_1\partial_1(u^1+u^2) = 0,\\ &\mathrm{i}\omega u^2 - A_2\partial_2(u^1+u^2) = 0, \end{aligned} \tag{23}$$

which can be obtained by substituting in Eq. (21), written in the frequency domain, the x_1 derivatives ∂_1 into $d(\omega,\zeta(x_1))\partial_1$, (see [16,17]), where

$$d(\omega,\zeta(x_1)) = \frac{\mathrm{i}\omega}{\zeta(x_1)+\mathrm{i}\omega}. \tag{24}$$

Actually, this corresponds to apply the complex change of variable [13,16,31],

$$x_1 \to x_1 + \frac{1}{\mathrm{i}\omega}\int_0^{x_1} \zeta(\xi)\mathrm{d}\xi,$$

to the solution of the frequency domain version of (21). The very astonishing property of this layer model is that it is perfectly matched, which means that it generates no reflection at the interface between the physical domain and the absorbing medium (see [17]). This property can be shown through a plane wave analysis. Furthermore, this analysis also shows that the transmitted wave decreases exponentially during its propagation inside the layer.

Of course to construct the PML model in the x_2 direction it suffices to permute the role of the space directions which gives the following system:

$$\begin{aligned} &\partial_t u^1 - A_1\partial_1(u^1+u^2) = 0,\\ &\partial_t u^2 + \zeta(x_2)u^2 - A_2\partial_2(u^1+u^2) = 0, \end{aligned} \tag{25}$$

and in a corner, the damping factor is introduced in both directions

$$\begin{aligned} &\partial_t u^1 + \zeta(x_1)u^1 - A_1\partial_1(u^1+u^2) = 0,\\ &\partial_t u^2 + \zeta(x_2)u^2 - A_2\partial_2(u^1+u^2) = 0. \end{aligned} \tag{26}$$

2.4. The PML model for elastodynamics

It is then straightforward to obtain the PML model for the elastodynamics system (9), that can be rewritten as

$$\begin{aligned} &\rho\frac{\partial v}{\partial t} - D^1\frac{\partial \sigma}{\partial x_1} - D^2\frac{\partial \sigma}{\partial x_2} = 0,\\ &A\frac{\partial \sigma}{\partial t} - E^1\frac{\partial v}{\partial x_1} - E^2\frac{\partial v}{\partial x_2} = 0, \end{aligned}$$

where

$$D^1 = \begin{pmatrix} 1 & 0 & 0\\ 0 & 0 & 1 \end{pmatrix}, \quad D^2 = \begin{pmatrix} 0 & 0 & 1\\ 0 & 1 & 0 \end{pmatrix}, \quad E^1 = \begin{pmatrix} 1 & 0 & 0\\ 0 & 0 & 1/2 \end{pmatrix}^{\mathrm{t}}, \quad E^2 = \begin{pmatrix} 0 & 0 & 1/2\\ 0 & 1 & 0 \end{pmatrix}^{\mathrm{t}}.$$

The PML system is then obtained by splitting $\sigma = \sigma^1 + \sigma^2$ and $v = v^1 + v^2$ (see [17]):

$$\begin{aligned}
&\rho \frac{\partial v^1}{\partial t} + \zeta(x_1) v^1 - D^1 \frac{\partial}{\partial x_1}(\sigma^1 + \sigma^2) = 0,\\
&\rho \frac{\partial v^2}{\partial t} - D^2 \frac{\partial}{\partial x_2}(\sigma^1 + \sigma^2) = 0,\\
&A \frac{\partial \sigma^1}{\partial t} + \zeta(x_1) \sigma^1 - E^1 \frac{\partial}{\partial x_1}(v^1 + v^2) = 0,\\
&A \frac{\partial \sigma^2}{\partial t} - E^2 \frac{\partial}{\partial x_2}(v^1 + v^2) = 0.
\end{aligned} \tag{27}$$

In the frequency domain, this system can be written in u as

$$\begin{aligned}
&\rho \omega^2 u + \mathrm{div}_{pml}\sigma(u) = 0,\\
&\sigma(u) = C\varepsilon_{pml}(u),
\end{aligned} \tag{28}$$

which is the same model as in the physical domain, substituting the operators div and ε with div_{pml} and ε_{pml}, where

$$\mathrm{div}_{pml}\sigma = \begin{pmatrix} d(\omega, \zeta(x_1))\partial_1\sigma_{11} + \partial_2\sigma_{12} \\ d(\omega, \zeta(x_1))\partial_1\sigma_{12} + \partial_2\sigma_{22} \end{pmatrix},$$

$$\varepsilon_{pml}(u) = \begin{pmatrix} d(\omega, \zeta(x_1))\partial_1 u_1 & \frac{1}{2}(d(\omega, \zeta(x_1))\partial_1 u_2 + \partial_2 u_1) \\ \frac{1}{2}(d(\omega, \zeta(x_1))\partial_1 u_2 + \partial_2 u_1) & \partial_2 u_2 \end{pmatrix}.$$

The PML model in the x_2 direction still has the general form (28) but this time

$$\mathrm{div}_{pml}\sigma = \begin{pmatrix} \partial_1\sigma_{11} + d(\omega, \zeta(x_2))\partial_2\sigma_{12} \\ \partial_1\sigma_{12} + d(\omega, \zeta(x_2))\partial_2\sigma_{22} \end{pmatrix},$$

$$\varepsilon_{pml}(u) = \begin{pmatrix} \partial_1 u_1 & \frac{1}{2}(\partial_1 u_2 + d(\omega, \zeta(x_2))\partial_2 u_1) \\ \frac{1}{2}(\partial_1 u_2 + d(\omega, \zeta(x_2))\partial_2 u_1) & d(\omega, \zeta(x_2))\partial_2 u_2 \end{pmatrix}.$$

2.5. Some instructive numerical simulations

In this section, we will show some simulations with four different homogeneous media, one is isotropic and the three others are orthotropic. The computational domain is a square 25 m × 25 m surrounded with PMLs of lenght $\delta = 5$ m so that the total computational domain is 35 m × 35 m (see Fig. 3, left). The numerical method used to solve the elastodynamic equations is based on a first-order original mixed formulation of the equations, described in [14], where the unknowns are the displacement searched in H^1 and some new vectorial unknowns searched in $(L^2)^2$. Since we are not interested here in the effects of the numerical scheme, but in the properties of the continuous model, we have also checked these results with another method, developed in [8,9] and still based on the velocity-stress formulation, but with v in L^2 and σ in $H(\mathrm{div})$.

In all the simulations, the initial data are taken equal to zero and the source is introduced as a right-hand side in Eq. (3)

$$f(x,t) = h(t)g(|x - x_S|)\vec{e}_1, \tag{29}$$

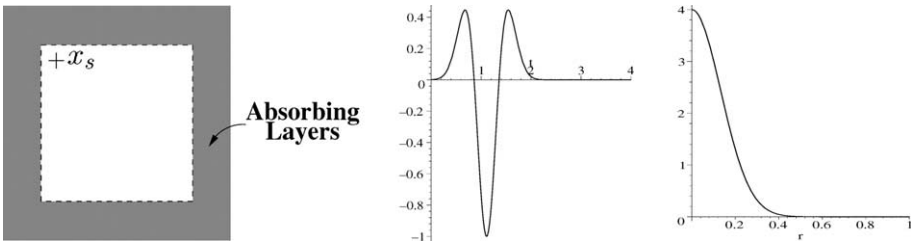

Fig. 3. Computational domain (left); function $h(t)$ (center); function $g(r)$ (right).

where $\vec{e}_1$ denotes the first vector of the canonical basis of $\mathbb{R}^2$ and h is the so-called second-order Ricker signal with central frequency equal to $f_0 = 0.9$ Hz, namely (see also Fig. 3)

$$h(t) = [2\pi^2(f_0 t - 1)^2 - 1]\mathrm{e}^{-\pi^2(f_0 t-1)^2}, \tag{30}$$

and the function $g(r)$ is the Gaussian function defined by (see Fig. 3)

$$g(r) = \frac{\mathrm{e}^{-7(r/r_0)^2}}{r_0^2}, \tag{31}$$

which is concentrated in a small disk of radius $r_0 = 0.5$ m. In our experiments, the source point x_S is located closed to the absorbing layer (2 m away from each layer) (see Fig. 3). We choose the density $\rho = 1$ kg m^{-3} in all experiments and give the elasticity coefficients in Pa. The damping factor is chosen as follows:

$$\zeta(x) = \frac{3c}{2\delta^3}\log(1/R)x^2, \tag{32}$$

where $R = 10^{-3}$ is the theoretical reflexion coefficient from the terminating reflection boundaries (see [17]) and $c = 4.5$ m s^{-1} is an upper bound of the wave velocities in all the considered materials.

We represent, for each experiment:

(a) the slowness curves and the wave fronts of the material,
(b) the distribution in space of the norm of the displacement field (snapshots) at several times.

Isotropic medium. The first simulation is done in an isotropic medium, with Lamé's constants

$$\lambda = 16, \quad \mu = 2. \tag{33}$$

The slowness curves and wave fronts are, here, circles (see Fig. 4). The source creates both P and S waves (of respective velocities $2\sqrt{5} \simeq 4.47$ and $\sqrt{2} \simeq 1.414$) that correspond to the two successive wavefronts appearing in the snapshots of the solution. One can see that these two waves are perfectly absorbed by the absorbing layer and that, even after a long while ($t = 500$ s), the solution remains equal to zero (see Fig. 8).

Simulation in an anisotropic medium (I). In this example, the elasticity coefficients are given by

$$c_{11} = 4, \quad c_{22} = 20, \quad c_{33} = 2 \quad \text{and} \quad c_{12} = 3.8. \tag{34}$$

The slowness curves and wave fronts reprensented in Fig. 5 illustrate the anisotropy of the medium. Note that the sets enclosed by the slowness curves remain convex as in the isotropic case. The snapshots of the corresponding numerical experiment are given in Fig. 9.

They show that the PMLs work pretty well. In particular, they are stable: the solution does not blow up, even after a long time.

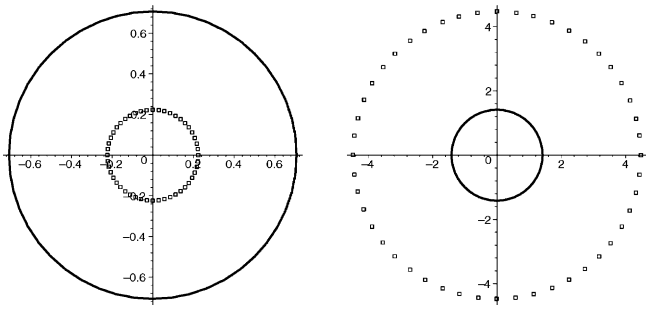

Fig. 4. Slowness curves and wave fronts for the isotropic media.

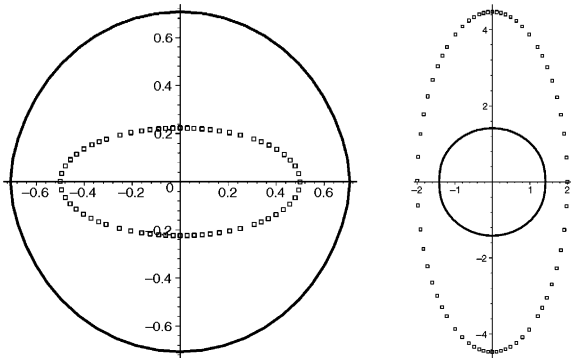

Fig. 5. Slowness curves and wave fronts for the orthotropic medium (I).

Simulation in an anisotropic medium (II). This time, the material is characterized by its elasticity coefficients

$$c_{11} = c_{22} = 20, \quad c_{33} = 2, \quad c_{12} = 3.8. \tag{35}$$

In Fig. 6, the medium appears to be much more anisotropic than the previous one. In particular, the set enclosed by the slowness curve of the QS wave is no longer convex, which gives rise to triplications of the wave front. However, one can see in Fig. 10 that the PML model still works very well and does not lead to any instability.

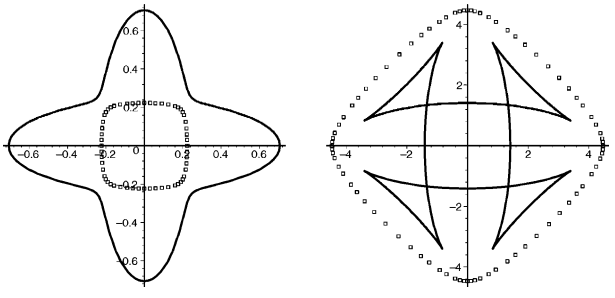

Fig. 6. Slowness curves and wave front for the orthotropic medium (II).

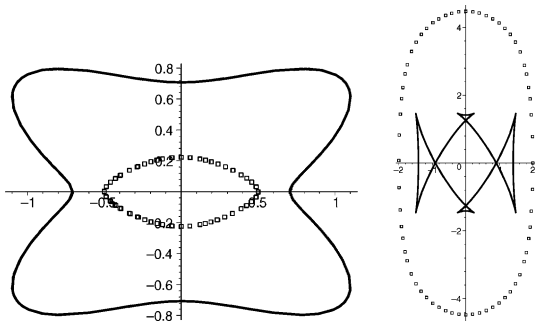

Fig. 7. Slowness curves and wave front for the orthotropic media (III).

Simulation in an anisotropic medium (III). Our last medium is characterized by the following elasticity coefficients:

$$c_{11} = 4, \quad c_{22} = 20, \quad c_{33} = 2, \quad c_{12} = 7.5. \tag{36}$$

Once again, this is a medium which gives rise to triplications of the QS wave front (see Fig. 7).

On the snapshots (see Fig. 11), we can see two instabilities appearing very soon in the two PML layers. These instabilities clearly occur when the lowest wave, namely the QS wave, penetrates the absorbing layer.

In conclusion, it seems that the stability of the PML model depends on the physical properties of the media. The aim of this paper is to understand this phenomenon. The explanation of the instabilities observed in the last simulation, is that this model does not satisfied a very general necessary condition of stability for the PMLs. This necessary condition has a very simple geometrical interpretation that we present in the following section.

3. A necessary stability condition for PML models associated to general hyperbolic system: interpretation in terms of slowness curves

In this section, we analyze the PML model (22) (or (25)) for a general hyperbolic system. We will make the following assumption:

Assumption (A_1). The unsplitted system (21) is strongly hyperbolic.

We restrict ourselves to the case where the absorption coefficient ζ is constant in space, which makes possible the use of the Fourier analysis. This is necessary step towards the analysis of the non-constant coefficient case. Moreover, there is a general theory for the link between the analysis of the constant coefficient equation and the one of variable coefficient equation. This is the so-called frozen coefficient technique (see [26]).

3.1. Well-posedness and stability: definition and characterization through plane wave analysis

We consider the Cauchy problem in the whole space $\mathbb{R}^2$ associated to the system

$$\begin{aligned} &\partial_t u^1 + \zeta u^1 - A_1 \partial_1 u^1 - A_1 \partial_1 u^2 = 0, \\ &\partial_t u^2 - A_2 \partial_2 u^1 - A_2 \partial_2 u^2 = 0, \end{aligned} \tag{37}$$

where ζ is a strictly positive constant and we set $U = (u^1, u^2)$.

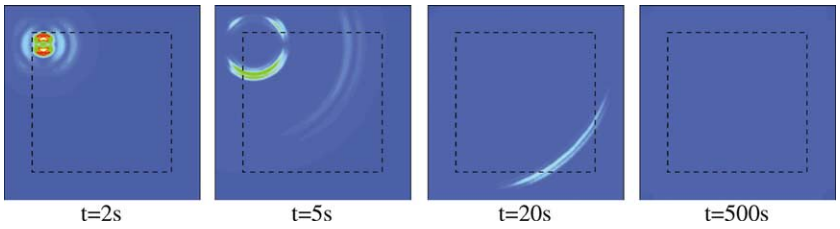

Fig. 8. Some snapshots at different times for the isotropic media.

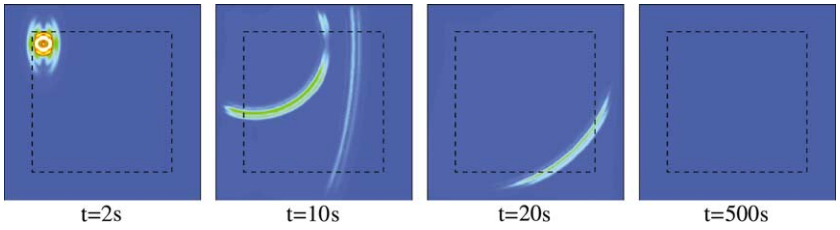

Fig. 9. Some snapshots at different times for the orthotropic medium (I).

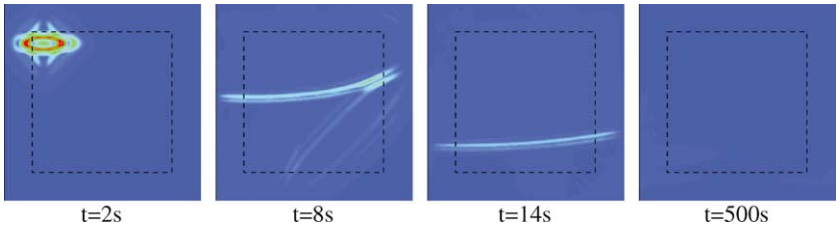

Fig. 10. Some snapshots at different times for the orthotropic medium (II).

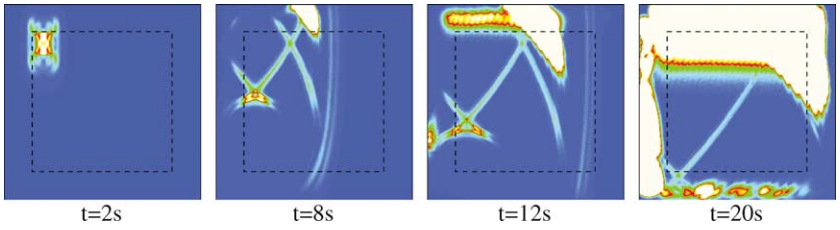

Fig. 11. Some snapshots at different times for the orthotropic media (III).

Definition 1. We will say that the Cauchy problem (37) associated to the initial data U_0 is weakly (resp. strongly) well-posed if for any $U(.,0) = U_0$ given in the Sobolev space H^s, $s > 0$ (resp. $s = 0$), (37) admits a unique solution $U(t)$ that satisfies an estimate on the type

$$\|U(.,t)\|_{L^2} \leqslant K e^{\alpha t} \|U_0\|_{H^s}. \tag{38}$$

We will say that the problem is *weakly* (*resp. strongly*) *stable* if it is weakly (or strongly) well-posed and if the solution $U(t)$ satisfies an estimate on the type

$$\|U(.,t)\|_{L^2} \leqslant K(1+t)^s \|U_0\|_{H^s} \tag{39}$$

with $s > 0$ (resp. $s = 0$).

In what follows we will say that the system is *stable* if it is at least weakly stable. Roughly speaking the difference between a stable system and a well-posed system is that in the first case, exponentially growing solutions are not permitted.

It is well known that the Fourier analysis permits to relate the notions of well-posedness and stability in terms of analysis of plane waves, i.e., solutions of the form

$$U(x,t) = \mathrm{e}^{\mathrm{i}(\omega t - k.x)} D, \quad k \in \mathbb{R}^2, \ D \in \mathbb{R}^{2m}, \ \omega \in \mathbb{C}. \tag{40}$$

To study such solutions it is useful to refer to the initial hyperbolic system (21)

$$\partial_t u - A_1 \partial_1 u - A_2 \partial_2 u = 0,$$

that admits plane wave solutions of the form

$$u(x,t) = \mathrm{e}^{\mathrm{i}(\omega t - k.x)} d, \quad k \in \mathbb{R}^2, \ d \in \mathbb{R}^m, \ \omega \in \mathbb{C},$$

if and only if k and ω are related by the dispersion relation

$$F_1(\omega, k) = 0, \tag{41}$$

where

$$F_1(\omega, k) = \det(\omega I - k_1 A_1 - k_2 A_2), \tag{42}$$

is a homogeneous polynomial in ω and k of degree m.

If we consider (41) as an equation in ω, a consequence of the hyperbolicity of system (21) (Assumption (A_1)) is that the solutions of (41) are real:

$$\omega = \omega_j(k), \quad j = 1, \ldots, m \ \text{(the eigenvalues of } \mathscr{A}(k)).$$

Moreover, the functions $\omega_j(k)$ are homogeneous functions of degree 1. In the following, for the sake of simplicity, we will make the assumption:

Assumption (A_2). We assume that the unsplitted system (21) admits:

- N_e non-zero eigenvalues of order 1, $\omega_j(k) \neq 0, \forall k \neq 0 \ j = 1, \ldots, N_e$ ($\omega_j(k) \neq \omega_i(k)$ for $i \neq j$),
- the zero eigenvalue of order $\ell_0 = m - N_e$, $\omega_j = 0$, $j = N_e + 1, \ldots, m$.

The mode zero is a non-propagating mode, and we will call the other modes the *physical modes*. This leads to the following expression:

$$F_1(\omega, k) = \omega^{\ell_0} \prod_{j=1}^{N_e} (\omega - \omega_j(k)). \tag{43}$$

Remark 2. One of the main limitations in Assumption (A_2) is that we assume that the physical modes correspond to simple eigenvalues. As a consequence, the results of this section are not directly applicable to 3D Maxwell's equations or isotropic elastodynamic equations. However, we think that this assumption only helps to simplify the technique of the proof (see Theorem 1) and conjecture that the well-posedness result remains true in the case of multiple non-zero eigenvalues.

Remark 3. For the elastic case, in 2D, we have seen in Section 2.2 that there were five modes: 0 of order $\ell_0 = 1$ and the physical modes $\pm\omega_{\mathrm{QP}}(k)$ and $\pm\omega_{\mathrm{QS}}(k)$, corresponding to two curves constituting the slowness curves. In most cases, Assumption (A_2) is satisfied, i.e., as soon as $c_{33} \neq c_{11}$ and $c_{33} \neq c_{22}$. In these particular cases, for instance $c_{33} = c_{11}$, the two curves intersect at points corresponding to $K_2 = 0$. One can then think that the solutions $\omega_{\mathrm{QP}}(k)$ and $\omega_{\mathrm{QS}}(k)$ are not differentiable with respect to k anymore, which is a trouble for defining the group velocity. But in fact, we then have to define the two branches in another way such that after the intersection we "jump" to the other branch (i.e., the QP branch will not correspond to the larger velocity anymore). This is illustrated with Fig. 12: left, this is the way we defined the two branches here, and right the way we should define it. Here again we think that we could apply the same type of analysis, but with additional technical difficulties.

As a consequence of Assumption (A_2), the physical modes $\omega(k) = \omega_j(k),\ j = 1, N_e$, are differentiable with respect to k, and, as for elastic waves, one can define for each mode, the phase velocity

$$\mathscr{V}(K) = \frac{\omega(k)}{|k|} \equiv \omega(K), \tag{44}$$

where $K = k/|k|$, the slowness vector

$$\vec{\mathscr{S}}(K) = \frac{K}{\mathscr{V}(K)} = \frac{k}{\omega(k)}, \tag{45}$$

and the group velocity

$$V_{\mathrm{g}}(k) = V_{\mathrm{g}}(K) = \nabla_k \omega(k) = -\left(\frac{\partial F_1}{\partial \omega}(\omega(k), k)\right)^{-1} \nabla_k F_1(\omega(k), k) \tag{46}$$

which is orthogonal to the slowness curves, defined as in Section 2. We shall denote by $(V_{\mathrm{g}}^1(k), V_{\mathrm{g}}^2(k))$ the two components of $V_{\mathrm{g}}(k)$ and by $(S_1(k), S_2(k))$ the ones of $\vec{\mathscr{S}}(K)$.

Going back to the Fourier analysis of the PML system (37), we see that (37) has solutions of the form (40) if and only if ω and k are related by the perturbed dispersion relation

$$F_{pml}(\omega, k, \zeta) \equiv F_1(\omega(\omega - \mathrm{i}\zeta), k_1\omega, k_2(\omega - \mathrm{i}\zeta)) = 0. \tag{47}$$

This is a polynomial equation in ω of degree $2m$. Therefore the dispersion relation in the PMLs defines $2m$ modes, $\omega_j(k, \zeta),\ j = 1, \ldots, 2m$, solutions of this equation. It is natural that the number of modes is the double of the one in the original problem, since we have doubled the number of unknowns by passing from (21) to (22).

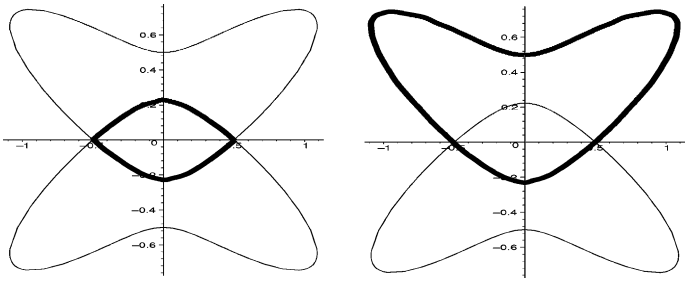

Fig. 12. Slowness diagrams of a material of coefficients $c_{11} = c_{33} = 4,\ c_{22} = 20,\ c_{12} = 7.5$. Left: in bold, the QP branch as it has been defined in (16). Right: in bold, the new definition of the "QP" branch.

We remind how the notions of well-posedness and stability are intimately related to the plane wave analysis.

Well-posedness. System (37) is *strongly ill-posed* if there exists some exponentially growing modes, i.e.,

$$\Im m\,\omega(k,\zeta) \to -\infty, \quad \text{when } |k| \to +\infty, \tag{48}$$

otherwise it is at least *weakly well-posed* (see [26]).

Stability. System (37) is *stable* in the sense of Definition 1 if and only if

$$\forall k \in \mathbb{R}^m, \text{ the solutions } \omega(k,\zeta) \text{ satisfy } \Im m\,\omega(k,\zeta) \geqslant 0. \tag{49}$$

Actually if $\omega = \omega_R + \mathrm{i}\omega_I$, the plane wave solution can be written as

$$u(x,t) = \mathrm{e}^{-\omega_I t}\mathrm{e}^{\mathrm{i}(\omega_R t - k.x)}D.$$

The existence of solutions ω with negative imaginary parts would correspond to plane wave solutions with exponential growth in time. A *stable* system does not admit such solutions.

3.2. A general well-posedness result

We can show the

Theorem 1. *We make Assumptions* (A_1) *and* (A_2) *for system* (21). *Then system* (37) *is well posed.*

According to (48), this theorem can be proved with a high frequency analysis, which will be also useful in the following, for deriving a necessary stability condition. More precisely, to prove the well-posedeness of (37), we will show that $\Im m\,\omega(k,\zeta)$ is bounded for large $|k|$ and therefore that (48) can never happen. For this, it will be convenient to introduce

$$\varepsilon = \frac{\zeta}{|k|}, \quad \mathscr{V}(K,\varepsilon) = \frac{\omega(k,\zeta)}{|k|}, \tag{50}$$

and to rewrite the dispersion relation (47) as

$$F_{pml}(\mathscr{V},K,\varepsilon) \equiv F_1(\mathscr{V}(\mathscr{V}-\mathrm{i}\varepsilon), K_1\mathscr{V}, K_2(\mathscr{V}-\mathrm{i}\varepsilon)) = 0, \tag{51}$$

where $K = k/|k|$ is the unit wave vector. We then have the

Lemma 1. *For every given* K, *Eq.* (51) *admits* $2m$ *complex solutions that we denote by* $(\mathscr{V}_j(K,\varepsilon))_{j=1,\ldots,2m}$, *that can be numbered in such a way that they are continuous functions with respect to* K *and* ε. *Moreover*, $(\mathscr{V}_j(K,\varepsilon))$ *is differentiable in the neighborhood of any point* (K_0,ε_0) *where* $(\mathscr{V}_j(K_0,\varepsilon_0))$ *is a simple root of* (51).

Proof. Using expression (43) of F_1, it is easy to see that the equation is a polynomial equation in the variable $\mathscr{V}$ of degree $2m$ and that the coefficient of order $2m$ in the polynomial function $F_{pml}(\mathscr{V},K,\varepsilon)$, equal to a power of i, does not vanish. Therefore the solutions $\mathscr{V}_j(K,\varepsilon)$ are continuous functions with respect to ε. The last part of the lemma results from the implicit function theorem. □

Note that looking at small ε is equivalent to looking at small ζ (small absorption) or large $|k|$ (high frequencies). The well-posedness is therefore related to the behavior of the solutions of the dispersion relation for small ε, so we first consider the limit case $\varepsilon = 0$.

The unperturbed equation. Eq. (51) is a perturbation of the equation obtained for $\varepsilon = 0$, which can be written as (F_1 is homogeneous of degree m):

$$F_{pml}(\mathscr{V},K,0)=\mathscr{V}^m F_1(\mathscr{V},K)=0. \tag{52}$$

The solutions $\mathscr{V}$ of this equation are:

- The N_e physical modes (of order 1)

$$\mathscr{V}_j(K,0)=\omega_j(K)=\omega_j(k)/|k|,\quad j=1,\dots,N_e. \tag{53}$$

- One mode of order $p\equiv m+\ell_0$,

$$\mathscr{V}_j(K,0)=0,\quad j=N_e+1,\dots,2m. \tag{54}$$

Proof of Theorem 1. We examine the solutions $\mathscr{V}_j(K,\varepsilon)$, $j=1,\dots,2m$, of (51) in the vicinity of the unperturbed modes defined in (53) and (54).

In the vicinity of a single root (*physical mode*). It is very easy to see that the ill-posedness cannot come from a single root, thanks to the implicit theorem. Actually, let $\mathscr{V}(K,0)\neq 0$ be a single root, then

$$\frac{\partial F_{pml}}{\partial \mathscr{V}}(\mathscr{V}(K,0),K,0)\neq 0$$

and the implicit theorem can be applied in the vicinity of $(\mathscr{V}(K,0),K,0)$. Therefore Eq. (51) defines a function $\mathscr{V}(K,\varepsilon)$ which is C^1 with respect to ε and thus which can be expanded as

$$\mathscr{V}(K,\varepsilon)=\mathscr{V}(K,0)+\varepsilon\alpha(K)+\mathrm{O}(\varepsilon^2). \tag{55}$$

This shows that

$$\omega(k,\zeta)=\omega(k)+\alpha(K)\zeta+\mathrm{O}(1/|k|). \tag{56}$$

Thus $\Im m\,\omega(k,\sigma)=\sigma\Im m\,\alpha(K)+\mathrm{O}(1/|k|)$ is bounded when $|k|\to+\infty$.

In the vicinity of the multiple mode $\mathscr{V}_j(K,0)=0$ of order $p=m+\ell_0$. Now let $\mathscr{V}(K,0)=0$ be the root of order p. Since the functions $\mathscr{V}_j(K,\varepsilon)$, $j=N_e+1,\dots,2m$, are continuous in ε and must vanish for $\varepsilon=0$, they admit a decomposition as a Puiseux series on the form [25]

$$\mathscr{V}_j(K,\varepsilon)=\alpha(K)\varepsilon^r+\mathrm{o}(\varepsilon^r)\quad\text{with } r\in\mathbb{Q}^+_{\star}. \tag{57}$$

If $r\geqslant 1$, it is clear from (50) that the corresponding $\omega_j(k,\zeta)$ have a bounded imaginary part. Let us assume that there exists a solution such that $0<r<1$ and $\alpha(K)\not\equiv 0$. Then, plugging (57) into the dispersion relation (51) yields

$$F_1(\alpha(K)^2\varepsilon^{2r}+\mathrm{o}(\varepsilon^{2r}),K_1\alpha(K)\varepsilon^r+\mathrm{o}(\varepsilon^r),K_2\alpha(K)\varepsilon^r+\mathrm{o}(\varepsilon^r))=0.$$

We now use the form of F_1 given by (43) that we rewrite as

$$F_1(\omega,k)=\omega^{\ell_0}\widetilde{F}_1(\omega,k)$$

with $\widetilde{F}_1(0,k)\not\equiv 0$, together with the homogeneity of F_1, to obtain

$$\begin{aligned}&(\alpha(K)\varepsilon^r)^{m+\ell_0}\widetilde{F}_1(\alpha(K)\mathrm{o}(\varepsilon^r),K_1+\mathrm{o}(1),K_2+\mathrm{o}(1))=0,\\ &\quad\Rightarrow(\alpha(K)\varepsilon^r)^{m+\ell_0}(\widetilde{F}_1(0,K_1,K_2)+\mathrm{o}(1))=0,\end{aligned}$$

which implies

$$\alpha(K)^{m+\ell_0}\widetilde{F}_1(0,K_1,K_2)=0.$$

Since $\widetilde{F}_1(0,K_1,K_2)$ cannot vanish for all K, this implies that $\alpha(K)=0$ which is in contradiction with (57). □

3.3. A high frequency stability analysis

For the general PML model, the stability condition (49) requires in particular that the high frequency solutions, i.e., $\omega(k,\zeta)$ for large $|k|$, have a positive imaginary part. This is what we call a high frequency necessary condition of stability:

Definition 2. System (37) is said to be *stable at high frequency* if and only if, there exists $\varepsilon_0>0$ such that

$$\forall \varepsilon<\varepsilon_0,\quad \forall K/|K|=1,\quad \Im m\,\mathscr{V}_j(K,\varepsilon)\geqslant 0,\quad j=1,\dots,2m. \tag{58}$$

We obtain in particular a necessary stability condition by writing that (58) holds for all physical modes ($j=1,\dots,N_e$). This allows us to prove the:

Theorem 2. *Let us suppose that system* (21) *satisfies Assumptions* (A_1) *and* (A_2). *A necessary condition of stability* (*high frequency stability*) *of the PML model in the* x_1 *direction* (37) *is that*, *for all physical modes of the unsplit system* (21):

$$\forall K=(K_1,K_2)/|K|=1,\quad S_1(K)\cdot(V_{\mathrm{g}}^1)_1\geqslant 0. \tag{59}$$

Proof. We have seen in the proof of Theorem 1 that in the vicinity of the physical modes, the function $\varepsilon\to\mathscr{V}(K,\varepsilon)=\mathscr{V}_j(K,\varepsilon)$ has an expansion of the form (55) (or equivalently (56)). Using the homogeneity of function F_1 and the fact that $\mathscr{V}(K,\varepsilon)$ cannot coincide with $i\varepsilon$, since we consider the physical modes, the dispersion relation (51) can be rewritten as

$$F_1\left(\mathscr{V}(K,\varepsilon),K_1\left(1-\mathrm{i}\frac{\varepsilon}{\mathscr{V}(K,\varepsilon)}\right)^{-1},K_2\right)=0.$$

Expanding this equality in powers of ε, using (55), we get

$$F_1(\mathscr{V}(K),K)+\varepsilon\alpha(K)\frac{\partial F_1}{\partial\omega}(\mathscr{V}(K),K)+i\varepsilon\frac{K_1}{\mathscr{V}(K)}\frac{\partial F_1}{\partial K_1}(\mathscr{V}(K),K)+\mathrm{O}(\varepsilon^2)=0,$$

By definition of $\mathscr{V}(K)$ one has $F_1(\mathscr{V}(K),K)=0$. Then, writing that the term in ε is equal to 0, we obtain

$$\alpha(K)=-\mathrm{i}\left(\frac{\partial F_1}{\partial\omega}(\mathscr{V}(K),K)\right)^{-1}\left(\frac{K_1}{\mathscr{V}(K)}\frac{\partial F_1}{\partial K_1}(\mathscr{V}(K),K)\right),$$

where we have used Assumption (A_2) which says that $\mathscr{V}(K)\neq 0$ and is a single eigenvalue, which implies that

$$\frac{\partial F_1}{\partial\omega}(\mathscr{V}(K),K)\neq 0.$$

Using formulas (46) and (45), we get

$$\alpha(K)=\mathrm{i}S_1(K)V_{\mathrm{g}}^1(K).$$

It is then easy to conclude since (55) shows that for small ε, the sign of $\Im m\, \mathcal{V}(K,\varepsilon)$ is given by the sign of $\Im m\, \alpha(K)$. A standard compactness argument is used to prove the existence of ε_0. □

Geometrical interpretation. Condition (59) expresses the fact that, along the slowness curves, the slowness vector and the group velocity are oriented in the same way with respect to the Ox_1 direction (cf. Fig. 13).

Obviously, when considering a PML model in the x_2 direction (i.e., parallel to the x_1 axis), one has the:

Corollary 1. *A necessary condition of stability* (*high frequency stability*) *of the PML model in the x_2 direction is that, for all physical modes of the unperturbed system* (21):

$$\forall K = (K_1, K_2)/|K| = 1, \quad S_2(K) \cdot V_g^2(K) \geqslant 0. \tag{60}$$

This result shows the importance of the role played by the group velocity in the stability analysis of PML models. This role has been first pointed out by Trefethen in [34] (see also [35,36]) for the stability analysis of finite difference schemes for linear hyperbolic systems and then by Higdon [23] for the well-posedness analysis of initial boundary value problems for linear hyperbolic systems. Concerning the stability analysis for PML models, we would like to mention [32] where the authors have related the instabilities observed with the PMLs for the linearized Euler equations to the existence of waves for which the group velocity and the phase velocity travel in opposite directions (see also Section 3.4.3).

3.4. Application of the geometrical stability criterion

3.4.1. Explanation of the observations of Section 2.5 via the analysis of slowness diagrams

The geometrical stability condition (59) is clearly satisfied in an isotropic medium. In this case, the slowness curves are composed of two circles and obviously the vectors $\vec{S}$ and V_g are parallel. More generally, it is easy to see that (59) will be satisfied as soon as the slowness curves are the boundary of convex sets, which is the case for the orthotropic material (I) considered in Section 2.5.

Concerning the two orthotropic materials (II) and (III) of Section 2.5, we have represented in Fig. 14 their slowness diagrams. The first remark is that for all the slowness curves associated to the QP waves (i.e., the inside curve), the geometrical condition is satisfied, since these curves are all convex. This is a general phenomenon that we will prove in the next Section (Lemma 3). Therefore, the violation of the high frequency stability condition can only come from the QS waves.

- For material (II), one can see that for all K, one has $V_1(K)S_1(K) \geqslant 0$ and $V_2(K)S_2(K) \geqslant 0$, therefore the high frequency stability condition is satisfied for a layer in the x_1 direction as well as for a layer in the x_2 direction. In this case, we did not observe any instability in the numerical results.

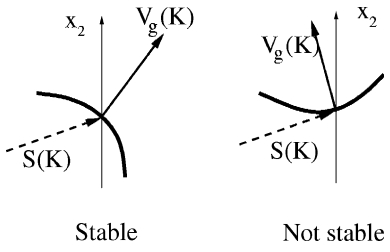

Fig. 13. Two different configurations. Left: the slowness vector $\vec{S}$ and the group velocity V_g are oriented in the same way with respect to the Ox_1 direction. Right: $\vec{S}$ and V_g are not oriented in in the same way with respect to the Ox_1 direction.

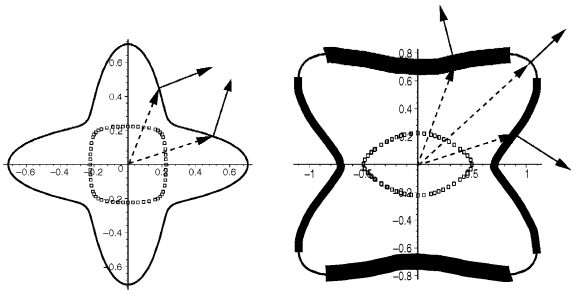

Fig. 14. Slowness diagrams. Left: material (II). Right: material (III).

- For material (III), there are some vectors K (whose extremities describe the thickest line in the figure) for which $V_1(K)S_1(K) < 0$ and there are some other vectors K (whose extremities describe the line of medium thickness on the figure) for which $V_2(K)S_2(K) < 0$ which means that the geometrical condition is not satisfied neither in x_1 nor in x_2. This also confirms the numerical results, since we observed instabilities in both layers.

3.4.2. Simulation in a whole absorbing domain

In this section, we make some simulations in a situation closed to the theoretical one: we consider a domain entirely composed by an absorbing layer, i.e., in which we solve the PML system with constant damping factor. Our aim is to illustrate the exponential blow up of the solution in the case of unstable medium.

We consider two materials: (II) and (III) (defined in Section 2.5). According to the geometrical criterion, the first medium is stable whereas the second one is unstable for high frequencies in the vicinity of the physical eigenvalues. So, for each material, we are interested in two experiments: we consider a 35 m $\times$ 35 m computational domain, in which we solve the PML model associated to the considered material respectively in the x_1 direction (22) for the first experiment, and in the x_2 direction (25) for the second one, with reflecting boundaries all around the domain. The pulse is defined by (29)–(31) but the source point is now located at the center of the computational domain. In the two cases, the absorbing coefficients are constants equal to 2.6.

Experiments in material (II). We first consider the material (II), whose elastic coefficients are defined in (35). The experiment with absorbing coefficient in the x_1 direction gives the snapshots in Fig. 15. One can observe that the part of the energy propagating in the x_1 direction is well absorbed. After a while, the wave can be considered as a plane wave only propagating in the x_2 direction. This explains then the low decay of the energy. No blow up is noticed.

The same remarks can be made in the second experiment (Fig. 16): the PML works pretty well for the part of the energy propagating in the x_2 direction and, after a while, the wave can be considered as a plane wave only propagating in the x_1 direction. Again, no blow up is noticed.

Experiments in material (III). The elastic coefficients are defined in (36). The first simulation, with absorbing factor in the x_1 direction, gives us the snapshots in Fig. 17. We observe that the solution blows up before reaching the external Dirichlet boundary.

We now represent the L^2 norm of the displacement field as a function of time in cartesian and semi-log axis (see Fig. 19). One observes that, for $t > 15$ s, the norm fits with the exponential function $e^{0.45t}$. We have checked that the solution we compute is stable with respect to mesh refinement which confirms the fact that the instability is due to the continuous problem and not to the discrete scheme.

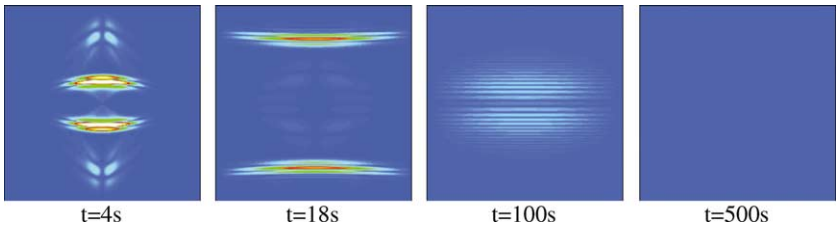

Fig. 15. Some snapshots at different times for the orthotropic medium (II) with only x_1 PML.

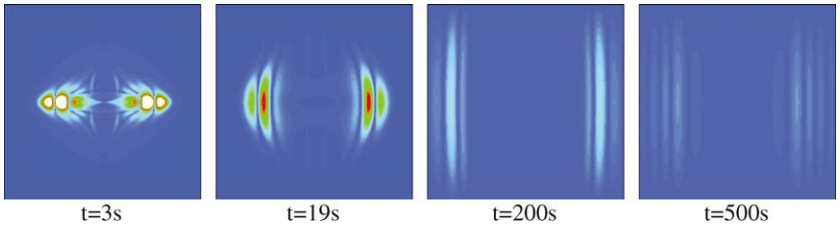

Fig. 16. Some snapshots at different times for the orthotropic medium (II) with only x_2 PML.

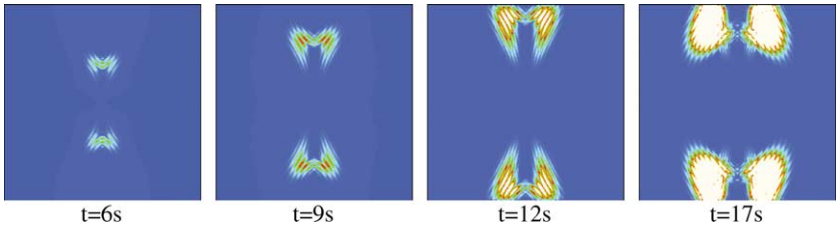

Fig. 17. Some snapshots at different times for the orthotropic medium (III) with only x_1 PML.

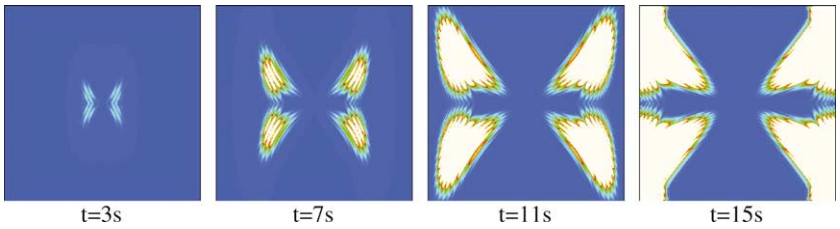

Fig. 18. Some snapshots at different times for the orthotropic medium (III) with only x_2 PML.

The second simulation, with absorbing factor in the x_2 direction, gives the snapshots in Fig. 18. In this case, the increasing of the solution is even faster than in the previous one, which is not surprising since the curvature of the part of the S slowness curve which gives rise to instabilities for a PML in x_2 is even stronger than the one in x_1.

Again if we represent the L^2 norm of the displacement field as a function of time in cartesian and semi-log axis (see Fig. 20), we observe that for $t > 15$ s, the norm fits with the exponential function $e^{0.65t}$. Note that the slope here (0.65) is larger than in the x_1 case (0.45) which confirms our previous remark.

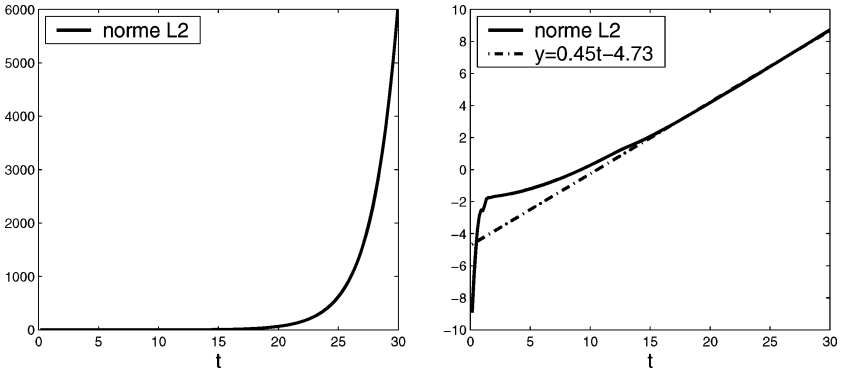

Fig. 19. Norm of the displacement field (left) and logarithm of the norm (right) for the orthotropic medium (III) with only x_1 PML.

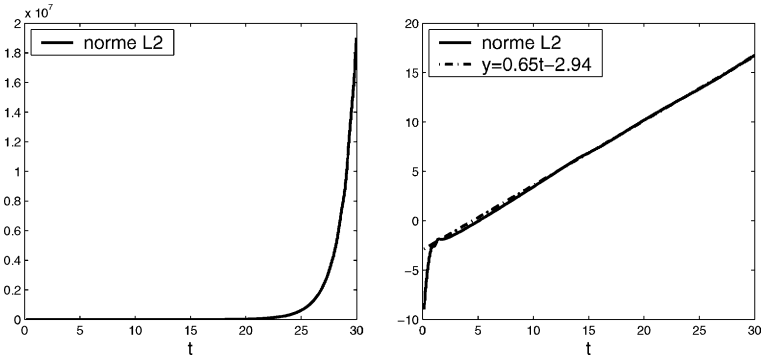

Fig. 20. Norm of the displacement field (left) and logarithm of the norm (right) for the orthotropic medium (III) with only x_2 PML.

Remark 4. In Section 3, we have established a necessary condition of stability and bring out a coefficient called α which corresponds to the exponential growth of the norm of the displacement field for high frequencies, in the vicinity of the physical eigenvalues. The simulations are not done exactly in the same framework than the theoretical one. Actually the source does not generate a plane wave with a given frequency, but a superposition of plane waves of a large range of frequencies. Therefore, the exponential growth is probably not produced only by the "high frequencies", which explains why the theoretical coefficient α does not fit the numerical observed coefficient in the exponential.

3.4.3. Application to other mathematical models

In this section, we show how our geometrical criterion can be applied to show the instability of the PML model applied to other wave phenomena.

The PML model for anisotropic electromagnetic waves. Anisotropic dielectric media are characterized by the fact that the electric permittivity ε is a tensor which is not necessarily proportional to the identity. In 2D, the propagation of electromagnetic waves in such a medium can be describes through the solution $u(x,t)$ of an anisotropic wave equation of the form

$$\frac{\partial^2 u}{\partial t^2} - \operatorname{div}(A\nabla u) = 0,$$

where A is a 2×2 symmetric positive definite matrix

$$A = \begin{pmatrix} a & b \\ b & c \end{pmatrix}, \quad a > 0, \ c > 0, \ ac - b^2 > 0.$$

It appears that the PML model associated to this equation is unstable as soon as the eigenvectors of the matrix A are not parallel to the coordinate axes, i.e. as soon as $b \neq 0$. Indeed, the dispersion relation can be written

$$\omega^2 = Ak \cdot k, \tag{61}$$

from which one deduces that the corresponding slowness diagramm is an ellipse whose axes are not parallel to the x_1 and x_2 axes. Fig. 21 illustrates the fact that the geometrical criterion (59) is not satisfied (this is moreover true for both x_1 and x_2 PML layers).

Fig. 22 gives an illustration of such an instability: we consider an unbounded anisotropic domain modeled by a square surrounded by PML. A is given by

$$a = \frac{3}{4}, \quad b = \frac{3}{2}, \quad c = 4.$$

The numerical method is quite the same as in the elastic case: we use a mixed formulation of the equation [14] and consider an explosive source at the middle of the square

$$f(x,t) = h(t)g(|x - x_S|),$$

where g and h have already been defined in Section 2.5. The central frequency is equal to 1 Hz.

The linearized Euler equations. We consider a fluid in which the sound speed is equal to 1 and look at the particular case of a uniform subsonic flow in the direction x_1 with Mach number $0 \leqslant M < 1$. The linearisation of Euler equations in the neighborhood of such a flow leads to the following advective wave equation which governs the acoustic propagation in such a situation (p denotes the pressure and $v = (v_1, v_2)$ is the velocity field)

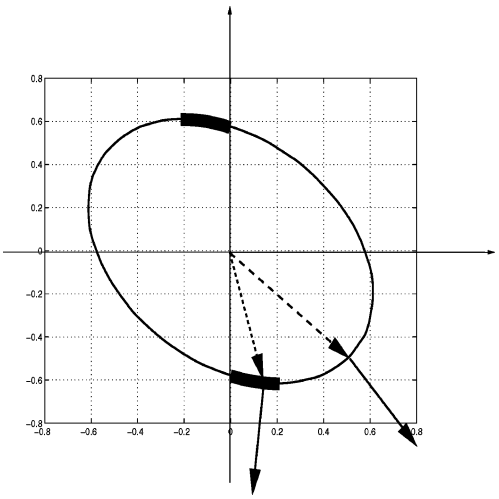

Fig. 21. The slowness curve for the anisotropic wave equation.

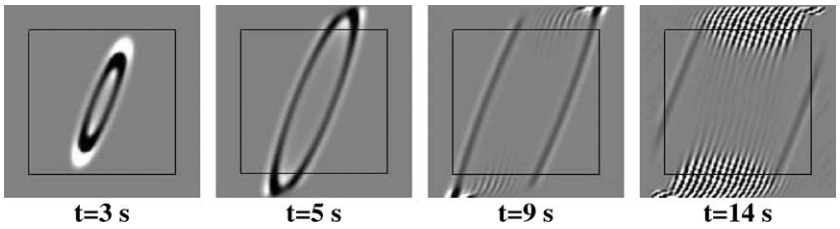

Fig. 22. Instability in the anisotropic acoustic case ($a = \frac{3}{4},\ b = \frac{3}{2},\ c = 4$).

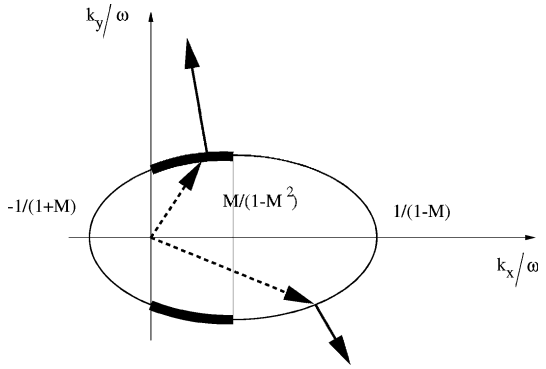

Fig. 23. The slowness curve for system (62).

$$\begin{aligned}
&\frac{\partial p}{\partial t} + M\frac{\partial p}{\partial x_1} - \frac{\partial v_1}{\partial x_1} - \frac{\partial v_2}{\partial x_2} = 0,\\
&\frac{\partial v_1}{\partial t} + M\frac{\partial v_1}{\partial x_1} - \frac{\partial p}{\partial x_1} = 0,\\
&\frac{\partial v_2}{\partial t} + M\frac{\partial v_2}{\partial x_1} - \frac{\partial p}{\partial x_2} = 0.
\end{aligned} \tag{62}$$

The high frequency geometrical criterium (59) allows us to identify a well known result, namely the instability of the PMLs in the x_1 direction (e.g. [22,24,32]). Indeed, the dispersion relation of (62),

$$(\omega + Mk_1)\Big((\omega + Mk_1)^2 - k_1^2 - k_2^2\Big) = 0, \tag{63}$$

defines one slowness curve which is an ellipse with axes parallel to the coordinates axes but not centered at the origin: the center is $(M/(1-M^2), 0)$. As a consequence, one can see in Fig. 23 that there are some vectors K (corresponding to the part of the curve of medium thickness) for which $S_1(K)V_1(K) < 0$. Let us mention [32] in which the authors have also related the instabilities to the presence of these waves and [1,5,18,20] that propose some solutions to stabilize the PMLs.

Remark 5. One can however check that the necessary condition for the stability of the PMLs in the x_2 direction is satisfied. The complete calculations shows that the corresponding system is stable.

3.5. Other instability phenomena via numerical simulations

In this section, we present two numerical simulations that seem to indicate that the necessary stability condition (59) is not sufficient for the elastodynamics system. We denote by (IV) and (V) these experiments which are done in the two following materials:

$$\text{Material (IV)} \quad c_{11} = 10, \quad c_{22} = 20, \quad c_{33} = 6, \quad c_{12} = 2.5,$$
$$\text{Material (V)} \quad c_{11} = 30, \quad c_{22} = 6, \quad c_{33} = 1.5, \quad c_{12} = 9.9.$$

In Figs. 24 and 25, we represent the slowness diagrams (left) and the wave fronts (right). It is clear that the high frequency conditions (59) and (60) are satisfied for both x_1 and x_2 layers since the slowness curves are convex.

We consider the same experiment as in Section 3.4.2: a 35 m $\times$ 35 m computational domain, in which we solve the PML model in the x_1 direction for both materials (IV) and (V), with a constant damping coefficient equal to 2.6. The pulse is defined by (29)–(31) and the source point is located at the center of the computational domain.

The snapshots of the experiment (IV) are given in Fig. 26. At the beginning the x_1-PML absorbs very well the waves. But after a long while, an instability appears. If we represent the L^2 norm of the displacement field with respect to time in cartesian and semi-log axis (see Fig. 27), we observe that for $t > 150$ s, the norm fits with the exponential function $e^{0.04t}$.

For the second experiment, (V), the snapshots are given in Fig. 28. At the beginning, the energy decays, but after 80 s an instability also appears. We then represent the L^2 norm of the displacement field with

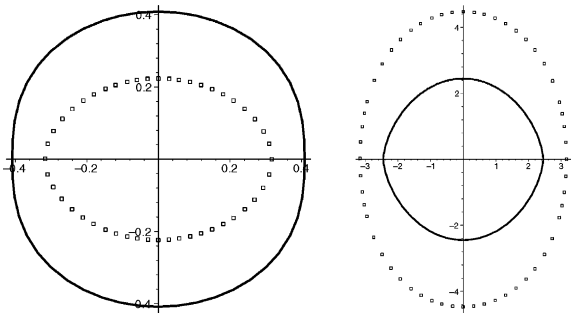

Fig. 24. Slowness curves and wave fronts in the medium (IV).

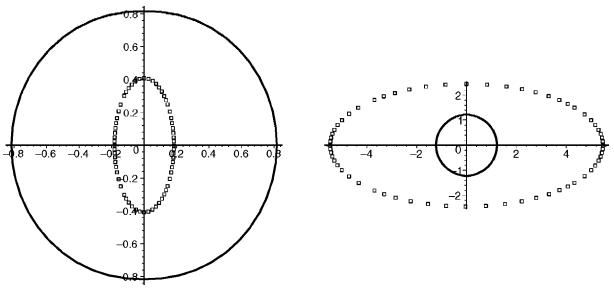

Fig. 25. Slowness curves and wave fronts in the medium (V).

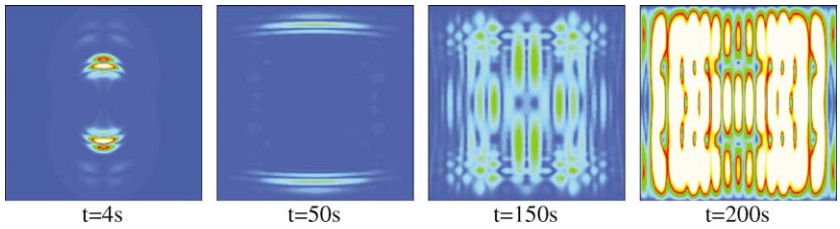

Fig. 26. Experiment (IV): some snapshots at different times for the orthotropic medium (IV) with only x_1 PML.

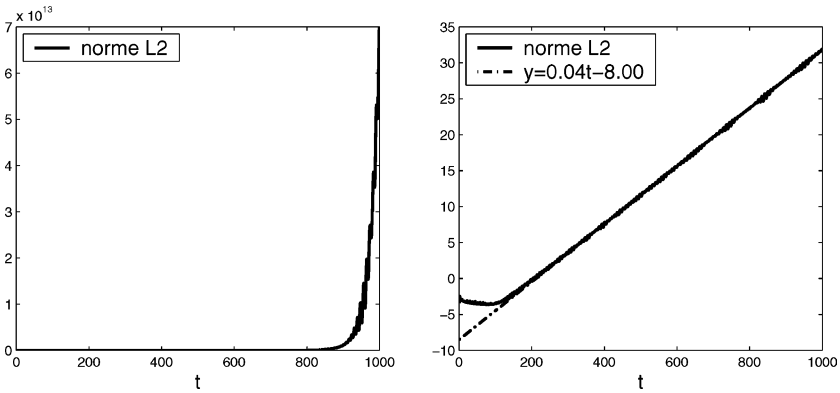

Fig. 27. Norm of the displacement field (left) and logarithm of the norm (right) for the orthotropic medium (IV) with only x_1 PML.

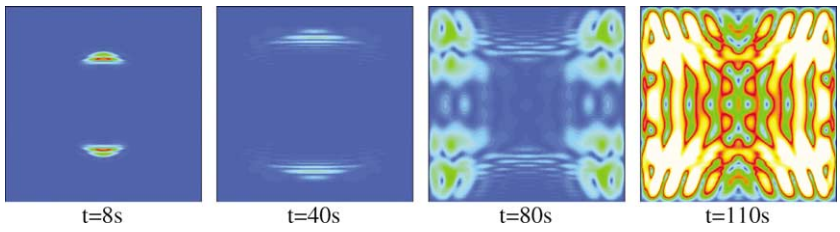

Fig. 28. Experiment (V): some snapshots at different times for the orthotropic medium (V) with only x_1 PML.

respect to time in cartesian and semi-log axis (see Fig. 29). For $t > 80$ s, the norm fits with the exponential function $e^{0.07t}$.

These kind of instabilities are only developing after a long time. We can check that the exponential growth rates observed in Section 3.4.2 for geometrical instabilities ($e^{0.45t}$ for x_1-PML and $e^{0.65t}$ for x_2-PML) are much more important than the growth rates observed in experiments (IV) ($e^{0.04t}$) and (V) ($e^{0.07t}$).

This suggests additional analysis. We will establish in the following section:

- another necessary stability condition (Lemma 4 and Theorem 4),
- a sufficient stability condition (Theorems 5 and 6).

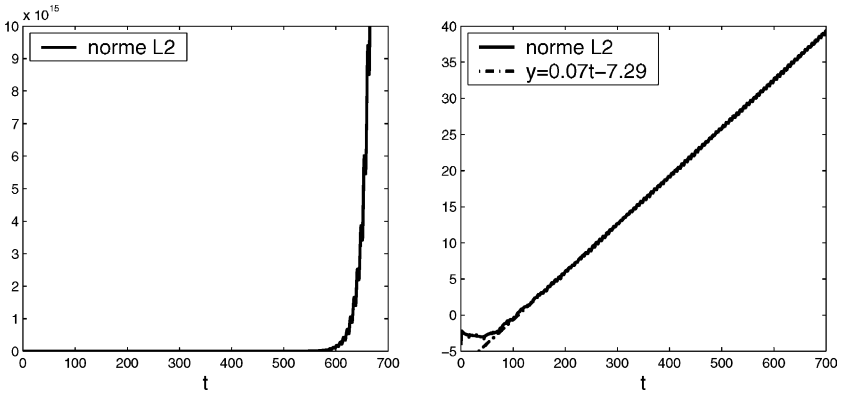

Fig. 29. Norm of the displacement field (left) and logarithm of the norm (right) for the orthotropic medium (V) with only x_1 PML.

4. Stability analysis for the orthotropic elastic model

We can now go back to the elastodynamic problem in 2D (1) and we consider the PML model in the whole space with a constant damping coefficient $\zeta > 0$. In this case $m = 5$ and the function F_{pml} appearing in the dispersion relation (47) can be rewritten, using (20), as

$$F_{pml}(\omega, k, \zeta) = \omega(\omega - \mathrm{i}\zeta)\det(\Gamma(\omega k_1, (\omega - \mathrm{i}\zeta)k_2) - \rho\omega^2(\omega - \mathrm{i}\zeta)^2 I) \equiv \omega(\omega - \mathrm{i}\zeta)\widetilde{F}_{pml}(\omega, k, \zeta). \tag{64}$$

Obviously the two modes $\omega = 0$ and $\omega = \mathrm{i}\zeta$ cannot give rise to any instability and in the following we will only concentrate on the eight modes associated to $\widetilde{F}_{pml}$. In Section 4.1, we will show how the high frequency necessary stability condition (59) (coming from the high frequency analysis in the vicinity of the four physical modes) can be expressed in terms of inequalities on the elasticity coefficients. In Section 4.2, we establish a second high frequency necessary stability condition, which comes from the analysis of the solutions in the vicinity of the multiple mode 0 of order 4.

The high frequency stability condition means that, for large k, the solutions $\omega(k, \zeta)$ are in the good side of the complex plane (i.e., with a positive imaginary part), but there is no guaranty that they stay in the good side for every frequencies. In Section 4.3, we obtain a condition which implies that the solutions never cross the real axis. Using a continuity argument, this allows to conclude that, under this condition, if the solutions are in the good side of the complex plane at high frequency, they necessarily stay in the good side for all frequencies. In this case, we get a sufficient stability condition. As in Section 3, we introduce the parameter $\varepsilon = \zeta/|k|$ and for convenience, we shall adopt a new notation by introducing the angle $\theta \in [-\pi, \pi[$ such that

$$K = \frac{k}{|k|} = (\cos\theta, \sin\theta).$$

Therefore, if we set

$$(\mathscr{V}_\theta)_j(\varepsilon) = \mathscr{V}_j(K, \varepsilon), \quad j = 1, \ldots, 8,$$

the functions $(\mathscr{V}_\theta)_j(\varepsilon)$ are the eigth branches of solutions of the dispersion relation, considered as an equation in the phase velocity $\mathscr{V}$ defined in (11):

$$\widetilde{F}_{pml}(\mathscr{V}, \theta, \varepsilon) \equiv \widetilde{F}_{pml}(\mathscr{V}, K, \varepsilon) = 0, \tag{65}$$

where $\widetilde{F}_{pml}$ has been defined in (64). We shall assume that the functions $(\mathscr{V}_\theta)_j(\varepsilon)$ are numbered in such a way that:

- $((\mathscr{V}_\theta)_j(\varepsilon))_{j=1,2}$, the two branches issued from the physical modes QP
$$(\mathscr{V}_\theta)_j(0) = \mathscr{V}_j(K,0) = \pm\omega_{\mathrm{QP}}(K), \quad j = 1,2.$$
- $((\mathscr{V}_\theta)_j(\varepsilon))_{j=3,4}$, the two branches issued from the physical modes QS
$$(\mathscr{V}_\theta)_j(0) = \mathscr{V}_j(K,0) = \pm\omega_{\mathrm{QS}}(K), \quad j = 3,4.$$
- $((\mathscr{V}_\theta)_j(\varepsilon))_{j=5,\ldots,8}$, the four branches issued from the multiple root of order 4
$$(\mathscr{V}_\theta)_j(0) = \mathscr{V}_j(K,0) = 0, \quad j = 5,\ldots,8.$$

It is easy to see that

$$\forall\theta \in [-\pi,\pi[, \quad \widetilde{F}_{pml}(\mathscr{V},\theta,\varepsilon) = \widetilde{F}_{pml}(\mathscr{V},-\theta,\varepsilon) = \widetilde{F}_{pml}(\mathscr{V},\pi-\theta,\varepsilon). \tag{66}$$

As a consequence, if

$$S(\theta,\varepsilon) = \{(\mathscr{V}_\theta)_j(\varepsilon), j = 1,\ldots,8\},$$

denotes the set of solutions of (65), one has

$$\forall\theta \in [-\pi,\pi[, \ \forall j = 1,\ldots,8, \quad S(\theta,\varepsilon) = S(-\theta,\varepsilon) = S(\pi-\theta,\varepsilon), \tag{67}$$

which justifies in what follows to restrict ourselves to

$$\theta \in [0,\pi/2].$$

The two limit values $\theta = 0$ and $\theta = \pi/2$ do not pose any problem as shown is the following (whose proof is immediate):

Lemma 2. *For $\theta = 0$, the solutions of* (65) *are given by*

$$\begin{aligned}
&(\mathscr{V}_0(\varepsilon))_{1,2} \equiv (\mathscr{V}_0(\varepsilon))^{\pm}_{\mathrm{QP}} = \pm\sqrt{max(c_{11},c_{33})} + \mathrm{i}\varepsilon, \ \textit{of order } 1,\\
&(\mathscr{V}_0(\varepsilon))_{3,4} \equiv (\mathscr{V}_0(\varepsilon))^{\pm}_{\mathrm{QS}} = \pm\sqrt{min(c_{11},c_{33})} + \mathrm{i}\varepsilon, \ \textit{of order } 1,\\
&((\mathscr{V}_0(\varepsilon))_j)_{j=5,\ldots,8} = 0, \ \textit{of order } 4.
\end{aligned} \tag{68}$$

For $\theta = \pi/2$, the solutions of (65) *are given by*

$$\begin{aligned}
&(\mathscr{V}_{\pi/2}(\varepsilon))_{1,2} \equiv (\mathscr{V}_{\pi/2}(\varepsilon))^{\pm}_{\mathrm{QP}} = \pm\sqrt{max(c_{22},c_{33})}, \ \textit{of order } 1,\\
&(\mathscr{V}_{\pi/2}(\varepsilon))_{3,4} \equiv (\mathscr{V}_{\pi/2}(\varepsilon))^{\pm}_{\mathrm{QS}} = \pm\sqrt{min(c_{22},c_{33})}, \ \textit{of order } 1.\\
&((\mathscr{V}_{\pi/2}(\varepsilon))_j)_{j=5,\ldots,8} = \mathrm{i}\varepsilon, \ \textit{of order } 4.
\end{aligned} \tag{69}$$

In particular $\Im m(\mathscr{V}_{\pi/2}(\varepsilon))_j \geqslant 0$ and $\Im m(\mathscr{V}_0(\varepsilon))_j \geqslant 0$, $j = 1,\ldots,8$.

It remains to consider $\theta \in]0,\pi/2[$.

4.1. A first high frequency necessary stability condition

We have established in Theorem 2 the high frequency necessary stability condition (59), which expresses the fact that, in the vicinity of the physical modes (i.e., for small ε), the branches of the solutions

$((\mathscr{V}_\theta)_j(\varepsilon))_{j=1,\dots,4}$ are in the good side of the complex plane (i.e., with a positive imaginary part). We give here an equivalent form of condition (59) expressed in terms of the elasticity coefficients.

Theorem 3. *The necessary condition of stability* (59) *is equivalent to*

$$(\mathscr{C}_1) \qquad \{(c_{12}+c_{33})^2 - c_{11}(c_{22}-c_{33})\} \times \{(c_{12}+c_{33})^2 + c_{33}(c_{22}-c_{33})\} \leqslant 0.$$

Proof. Since the proof is very technical, we omit it here but it can be found in [7], proof of Theorem 2 (p. 26). □

Theorem 3 means that, if $(\mathscr{C}_1)$ is satisfied, then one has for small ε:

$$\Im m((\mathscr{V}_\theta)_j(\varepsilon)) \geqslant 0 \quad \forall\theta \in]0,\pi/2[, \ \ \forall j = 1,\dots,4. \tag{70}$$

In the following lemma, we make the result more precize: we show that the instability cannot come from the vicinity of the QP waves, which is in some sense a theoretical confirmation of what we have observed in the numerical experiments of Section 2.

Lemma 3. *For any orthotropic material, one has the following property, for small* ε:

$$\Im m((\mathscr{V}_\theta)_j)(\varepsilon) \geqslant 0 \quad \forall\theta \in]0,\pi/2[, \ \ j = 1,2. \tag{71}$$

Proof. Again we omit the proof and refer to [7], proof of Lemma 3 (p. 27). □

4.2. A second high frequency necessary stability condition

We assume in this section that $\theta \in]0,\pi/2[$.

Lemma 4. *The four solutions* $(\mathscr{V}_\theta(\varepsilon))_j$, $j = 5,\dots,8$, *satisfy*

$$\Im m((\mathscr{V}_\theta^1)_j) \geqslant 0 \quad \forall\theta \in]0,\pi/2[, \ \ \forall j = 5,\dots,8, \tag{72}$$

if and only if the two following inequalities are satisfied:

$$(\mathscr{C}_2) \qquad \begin{cases} (c_{12}+2c_{33})^2 \leqslant c_{11}c_{22}, & \text{(i)} \\ (c_{12}+c_{33})^2 \leqslant c_{11}c_{22} + c_{33}^2. & \text{(ii)} \end{cases}$$

Proof. See Appendix A. □

Theorem 3 and Lemma 4 can be regrouped as follows:

Theorem 4. *The PML model* (28) *is stable at high frequency in the sense of Definition* 2 *if and only if conditions* $(\mathscr{C}_1)$ *and* $(\mathscr{C}_2)$ *are satisfied.*

4.3. A sufficient stability condition

From a geometrical point of view, proving the stability of the PML model is equivalent to show that, θ playing the role of a parameter, the curves in the complex plane described by $(\mathscr{V}_\theta)_j(\varepsilon)$ when ε

goes from 0 to $+\infty$ is located in the right side of the complex plane, namely the half-space of complex numbers with positive imaginary part. In the previous sections, we have established conditions $(\mathscr{C}_1)$ and $(\mathscr{C}_2)$ such that it is the case for the first part of the curves corresponding to small ε. In what follows, we are going to establish the conditions for which these curves never meet again the real axis, which will provide us a sufficient stability condition thanks to a continuity argument. The property which means that the curves $\varepsilon \mapsto \mathscr{V}_j(\varepsilon)$ never meet again the real axis, can be expressed as follows:

$$(P_1) \qquad \forall \theta \in]0, \pi/2[, \ \forall j = 1, \ldots, 8, \quad (\mathscr{V}_\theta(\varepsilon))_j \in \mathbb{R} \Rightarrow \varepsilon = 0.$$

Lemma 5. *The property (P_1) is realized if and only if the condition $(\mathscr{C}_2)$ (i) is satisfied as well as one of the two following conditions $(\mathscr{C}_3)_1$ or $(\mathscr{C}_3)_2$:*

$$(\mathscr{C}_3)_1 \qquad (c_{12} + c_{33})^2 \leqslant (c_{11} - c_{33})(c_{22} - c_{33}),$$
$$(\mathscr{C}_3)_2 \qquad (c_{11} + c_{33})(c_{12} + c_{33})^2 \geqslant (c_{11} - c_{33})(c_{11}c_{22} - c_{33}^2).$$

Proof. See Appendix B. □

Theorem 5. *A sufficient condition for the stability of the PML system* (28) *with absorption in the x_1 direction is that conditions $(\mathscr{C}_1)$ and $(\mathscr{C}_2)$ be satisfied as well as one of the conditions $(\mathscr{C}_3)_1$ or $(\mathscr{C}_3)_2$. This is equivalent to saying that one of the two following conditions is realized*:

$$(\mathscr{C}_{x_1})_1 \quad (c_{12} + c_{33})^2 < (c_{11} - c_{33})(c_{22} - c_{33}),$$
$$(\mathscr{C}_{x_1})_2 \quad \begin{cases} \text{(i)} & (c_{11} - c_{33})(c_{22} - c_{33}) \leqslant (c_{12} + c_{33})^2 \leqslant \max\{-c_{33}(c_{22} - c_{33}), c_{11}(c_{22} - c_{33})\}, \\ \text{(ii)} & (c_{11} - c_{33})\left(c_{11}c_{22} - c_{33}^2\right) < (c_{11} + c_{33})(c_{12} + c_{33})^2, \\ \text{(iii)} & (c_{12} + 2c_{33})^2 < c_{11}c_{22}. \end{cases}$$

Proof. It simply remains to explain why satisfying $(\mathscr{C}_1)$, $(\mathscr{C}_2)$ and $(\mathscr{C}_3)_1$ or $(\mathscr{C}_3)_2$ is equivalent to $(\mathscr{C}_{x_1})_1$ or $(\mathscr{C}_{x_1})_2$. We first observe that the two real numbers

$$-c_{33}(c_{22} - c_{33}) \quad \text{and} \quad c_{11}(c_{22} - c_{33})$$

have opposite signs. As a consequence, the maximum of these two values is positive and greater than their sum

$$(c_{11} - c_{33})(c_{22} - c_{33}) \leqslant \max\{-c_{33}(c_{22} - c_{33}), c_{11}(c_{22} - c_{33})\} \quad (\geqslant 0). \tag{73}$$

We next observe that condition $(\mathscr{C}_1)$ means that $(c_{12} + c_{33})^2$ belongs to the interval delimited by the same two numbers. Since $(c_{12} + c_{33})^2 > 0$, this reduces to

$$(c_{12} + c_{33})^2 \leqslant \max\{-c_{33}(c_{22} - c_{33}), c_{11}(c_{22} - c_{33})\}. \tag{74}$$

As $-c_{33}(c_{22} - c_{33}) \leqslant c_{33}^2$ and $c_{11}(c_{22} - c_{33}) \leqslant c_{11}c_{22}$, we deduce that

$$(74) \Rightarrow (c_{12} + c_{33})^2 \leqslant \max\left\{c_{33}^2, c_{11}c_{22}\right\} \leqslant c_{33}^2 + c_{11}c_{22},$$

in other words

$$(\mathscr{C}_1) \Rightarrow (\mathscr{C}_2) \quad \text{(ii)}. \tag{75}$$

The less immediate remark, whose proof is left to the reader, i.e.,

$$(c_{12}+c_{33})^2 \leqslant (c_{11}-c_{33})(c_{22}-c_{33}) \Rightarrow (c_{12}+2c_{33})^2 \leqslant c_{11}c_{22} \quad \text{(i.e., } (\mathscr{C}_2)\text{ (i))} \tag{76}$$

One then concludes as follows:

1. If $(\mathscr{C}_{x1})_1$ – which is nothing but $(\mathscr{C}_3)_1$ – $(\mathscr{C}_1)$ is satisfied thanks to (73) and (74). Therefore $(\mathscr{C}_2)$ (ii) holds thanks to (76) and $(\mathscr{C}_2)$ (i) holds thanks to (75). If $(\mathscr{C}_{x1})_2$ is satisfied, $(\mathscr{C}_1)$ (and thus $(\mathscr{C}_2)$ (ii)) results from $(\mathscr{C}_{x1})_2(i)$, $(\mathscr{C}_1)$ from $(\mathscr{C}_{x1})_2$ (iii) and $(\mathscr{C}_3)_2$ from $(\mathscr{C}_{x1})_2$ (ii).
2. Reciprocally, if $(\mathscr{C}_1)$, $(\mathscr{C}_2)$ and $(\mathscr{C}_3)_1$ or $(\mathscr{C}_3)_2$ are satisfied, then, according to (73) and (74) either

$$(c_{12}+c_{33})^2 < (c_{11}-c_{33})(c_{22}-c_{33})$$

in which case $(\mathscr{C}_{x1})_1$ holds, either

$$(c_{11}-c_{33})(c_{22}-c_{33}) \leqslant (c_{12}+c_{33})^2 \leqslant \max\{-c_{33}(c_{22}-c_{33}), c_{11}(c_{22}-c_{33})\},$$

i.e., $(\mathscr{C}_{x1})_2$ (i), in which case $(\mathscr{C}_{x1})_2$ (i) and $(\mathscr{C}_{x1})_2$ (i) result from $(\mathscr{C}_2)$(i) and $(\mathscr{C}_3)_2$ (which is satisfied since $(\mathscr{C}_3)_1$ is not). □

In order to obtain a sufficient condition for the stability for the PML model with absorption in the x_2 direction, we simply have to permute c_{11} and c_{22}:

Theorem 6. *The PML system* (28) *with absorption in the x_2 direction is stable as soon as one of the two following conditions is realized*:

$$(\mathscr{C}_{x_2})_1 \quad (c_{12}+c_{33})^2 < (c_{11}-c_{33})(c_{22}-c_{33}),$$

$$(\mathscr{C}_{x_2})_2 \quad \begin{cases} \text{(i)} & (c_{11}-c_{33})(c_{22}-c_{33}) \leqslant (c_{12}+c_{33})^2 \leqslant \max\{-c_{33}(c_{22}-c_{33}), c_{11}(c_{22}-c_{33})\}, \\ \text{(ii)} & (c_{22}-c_{33})\left(c_{11}c_{22}-c_{33}^2\right) < (c_{22}+c_{33})(c_{12}+c_{33})^2, \\ \text{(iii)} & (c_{12}+2c_{33})^2 < c_{11}c_{22}. \end{cases}$$

Remark 6. In the isotropic case, the coefficients are expressed in terms of Lamé's coefficients λ, μ through relation (8) one easily checks that condition $(\mathscr{C}_1)_{x_1} \equiv (\mathscr{C}_1)_{x_2}$ is obviously satisfied, therefore the PML model with absorption in x_1 or in x_2 is stable for any isotropic material.

Remark 7. Conditions (7) on the coefficients do not imply the positivity of coefficient c_{12}. However, in the applications this coefficient is often positive. It is easy to see that in this case, if $c_{33} > c_{22}$, the condition $(\mathscr{C}_1)$ cannot be satisfied, therefore the PML model with absorption in the x_1 direction is not stable. In the same way, if $c_{33} > c_{11}$, the PML model with absorption in the x_2 direction is not stable. Therefore, if $c_{12} \geqslant 0$, a necessary condition for the general PML model to be stable is that $c_{33} \leqslant c_{22}$ and $c_{33} \leqslant c_{11}$.

4.4. Back to the numerical experiments of Section 3.5

We come back to the numerical experiments done at Section 3.5. We have seen that both materials (IV) and (V) satisfy the geometrical stability condition. However, we can understand the instability phenomena observed in Figs. 26 and 28, thanks to the analysis in Sections 4.2 and 4.3. Indeed, one can check that

- The material (IV) satisfies the condition $(\mathscr{C}_3)$ but does not satisfy the necessary condition $(\mathscr{C}_2)$ that concerns the high frequency analysis of the non-physical modes.
- The material (V) satisfies the necessary condition $(\mathscr{C}_2)$ but does not satisfy the condition $(\mathscr{C}_3)$ that concerns the stability of the physical modes at intermediate frequencies.

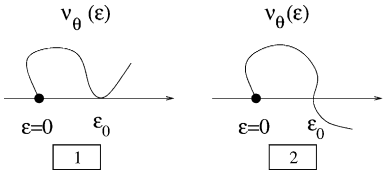

Fig. 30. The two possibilities for each curve $\mathscr{V}_\theta(\varepsilon)$.

Conjecture. We conjecture that the sufficient conditions of Theorems 5 and 6 are also necessary stability conditions. The idea is that, as soon as $(\mathscr{C}_3)_1$ or $(\mathscr{C}_3)_2$ is not satisfied, there exists $\theta_0 \in]0, \pi/2[$ such that one curve $\varepsilon \mapsto (\mathscr{V}_{\theta_0})_j(\varepsilon)$ meets the real axis for some $\varepsilon = \varepsilon_0 > 0$. The proof would be complete if one would be able to show that this curve really crosses the real axis at $\varepsilon = \varepsilon_0$ (case 2 of Fig. 30). This would essentially corresponds to proving that

$$\mathfrak{Im}\left\{ \frac{\partial}{\partial \varepsilon}(\mathscr{V}_{\theta_0})_j(\varepsilon_0) \right\} \neq 0,$$

that we have not been able to do.

Another element for this conjecture is, of course, the instabilities observed for the material (V) in Fig. 28.

Acknowledgements

The authors would like to thank the referees for their careful reading, corrections and helpful suggestions.

Appendix A. Proof of Lemma 4

In what follows, $\mathscr{V}_\theta(\varepsilon)$ is one of the functions $(\mathscr{V}_\theta)_j(\varepsilon)$ for $j = 5, \ldots, 8$. Let us substitute the expansion (we know that such an expansion exists since we have weak well-posedness)

$$\mathscr{V}_\theta(\varepsilon) = \varepsilon \mathscr{V}_\theta^1 + o(\varepsilon)$$

into the equation

$$F_{pml}(\mathscr{V}_\theta(\varepsilon), \theta, \varepsilon) = 0.$$

We obtain, by identifying the lower order term in ε:

$$\left[c_{11}(\mathscr{V}_\theta^1)^2 \cos^2\theta + c_{33}(\mathscr{V}_\theta^1 - i)^2 \sin^2\theta\right]\left[c_{33}(\mathscr{V}_\theta^1)^2 \cos^2\theta + c_{22}(\mathscr{V}_\theta^1 - i)^2 \sin^2\theta\right] - (c_{12} + c_{33})^2 \times (\mathscr{V}_\theta^1)^2(\mathscr{V}_\theta^1 - i)^2 \cos^2\theta \sin^2\theta = 0. \tag{A.1}$$

It is easy to see that for $\theta \in]0, \pi/2[$, the solution $\mathscr{V}_\theta^1$ does not vanish, then we can make the change of unknown

$$z = \frac{\mathscr{V}_\theta^1 - i}{\mathscr{V}_\theta^1} \tan\theta, \tag{A.2}$$

which leads to a polynomial equation in z whose coefficients are independent of θ:

$$A_4 z^4 + A_2 z^2 + A_0 = 0, \tag{A.3}$$

with

$$\begin{aligned} A_4 &= c_{22}c_{33} > 0, \\ A_2 &= c_{11}c_{22} + c_{33}^2 - (c_{12} + c_{33})^2, \\ A_0 &= c_{11}c_{33} > 0. \end{aligned} \tag{A.4}$$

Let us show the equivalence of the two following conditions:
(a) The solutions $\mathscr{V}_\theta^1$ of (A.1) have a positive imaginary part for all values of θ.
(b) The solutions z of (A.3) are purely imaginary.
Indeed, if (b) holds and if $\{\mathrm{i}\lambda_j,\ j = 5, \ldots, 8\}$ are the four roots of (A.3) then the four solutions of (A.1) are given by

$$(\mathscr{V}_\theta^1)_j = \frac{\mathrm{i}\tan\theta}{\tan\theta - \mathrm{i}\lambda_j} = \tan\theta \frac{-\lambda_j + \mathrm{i}\tan\theta}{\tan^2\theta + \lambda_j^2}$$

so that

$$\mathfrak{Im}(\mathscr{V}_\theta^1)_j = \frac{\tan^2\theta}{\tan^2\theta + \lambda_j^2} \geqslant 0.$$

Conversely, let us assume that z is a solution of (A.3) with non-zero real part (note that $z \neq 0$). We can assume that $\mathfrak{Re}(z) > 0$ since $-z$ is also a solution. Then, except maybe for $\theta = \theta_0$ such that, when z is real, $z = \tan\theta_0$, a solution of (A.2) is given by

$$\mathscr{V}_\theta^1 = \frac{\mathrm{i}\tan\theta}{\tan\theta - z} = \tan\theta \frac{-\mathfrak{Im}(z) + \mathrm{i}(\tan\theta - \mathfrak{Re}(z))}{|\tan\theta - z|^2}$$

with imaginary part

$$\mathfrak{Im}\,\mathscr{V}_\theta^1 = \frac{\tan\theta(\tan\theta - \mathfrak{Re}(z))}{|\tan\theta - z|^2}.$$

It suffices to remark that when θ goes from 0 to $\pi/2$ the sign of $\tan\theta - \mathfrak{Re}(z)$ changes which means that, for some values of θ, (A.3) admits solutions with strictly negative imaginary part.

To conclude, it suffices to remark that (a) is equivalent to saying that the two roots of the polynomial $A_4Z^2 + A_2Z + A_0$ are real negative, which is equivalent to

$$A_2^2 \geqslant 4A_0A_4 \quad \text{and} \quad A_2 \geqslant 0,$$

what we wanted to show since $c_{11}c_{22} - c_{12}^2 \geqslant 0$ and

$$A_2^2 - 4A_0A_4 = (c_{11}c_{22} - c_{12}^2)\left[c_{11}c_{22} - (c_{12} + 2c_{33})^2\right].$$

Appendix B. Proof of Lemma 5

For our purpose, it will be useful to use a new parameterization of the $(\theta, \mathscr{V}, \varepsilon)$ space. More precisely, we consider the transformation (we shall see that this transformation is one to one)

$$(\theta, \mathscr{V}, \varepsilon) \in \left]0, \frac{\pi}{2}\right[\times \mathbb{R}_* \times \mathbb{R}_*^+ \mapsto (X, \tau) \in \mathbb{R}_*^+ \times (\mathbb{C} \setminus \mathbb{R})$$

defined by (we set $t = \tan\theta$)

$$\begin{aligned} X(\theta, \mathscr{V}) &= \frac{1+t^2}{t^2}\mathscr{V}^2, \\ \tau(\theta, \varepsilon, \mathscr{V}) &= t^2\left(\frac{\mathscr{V} - \mathrm{i}\varepsilon}{\mathscr{V}}\right)^2. \end{aligned} \tag{B.1}$$

By construction, we have

$$\widetilde{F}_{pml}(\mathscr{V}, \theta, \varepsilon) = \cos^4\theta \mathscr{V}^4 G(X(\theta, \mathscr{V}), \tau(\theta, \varepsilon, \mathscr{V})) \tag{B.2}$$

with

$$G(X, \tau) = (c_{11} + (c_{33} - X)\tau)(c_{33} + (c_{22} - X)\tau) - (c_{12} + c_{33})^2\tau. \tag{B.3}$$

We then use this parametrization to express the property (P_1) in another way, by proving the:

Lemma 6. *The property* (P_1) *is equivalent to*

$$(P_2) \qquad \forall X \in \mathbb{R}^+, \quad g(X, \tau) = 0 \Rightarrow \tau \in \mathbb{R}.$$

Proof. For the proof of this lemma, we refer to [7], proof of Lemma 5 (p. 30). □

We now use the equivalence between (P_1) and (P_2) to prove the Lemma 5:

Proof of Lemma 5. Let us rewrite $G(X, \tau)$ as a polynomial of degree two with respect to τ:

$$G(X, \tau) = (c_{33} - X)(c_{22} - X)\tau^2 + (c_{11}(c_{22} - X) + c_{33}(c_{33} - X) - (c_{12} + c_{33})^2)\tau + c_{11}c_{33}.$$

Its discriminant is given by

$$\Delta(X) = \alpha_2 X^2 + 2\alpha_1 X + \alpha_0$$

with

$$\begin{aligned} \alpha_2 &= (c_{11} - c_{33})^2 \geqslant 0, \\ \alpha_1 &= (c_{11} + c_{33})(c_{12} + c_{33})^2 - (c_{11} - c_{33})(c_{11}c_{22} - c_{33}^2), \\ \alpha_0 &= (c_{11}c_{22} - c_{12}^2)(c_{11}c_{22} - (c_{12} + 2c_{33})^2). \end{aligned}$$

Obviously, we have the equivalence

$$(P_2) \Longleftrightarrow \Delta(X) \geqslant 0 \quad \forall X \geqslant 0.$$

This means that the two roots of $\Delta(X)$ are either non-real either negative, which is equivalent to

$$\alpha_0 \geqslant 0 \quad \text{(i.e. } (\mathscr{C}_2)\text{) and (i) or (ii)},$$

where

$$\begin{aligned} &\text{(i)} \quad \alpha_0\alpha_2 \geqslant \alpha_1^2, \\ &\text{(ii)} \quad \alpha_1 \geqslant 0 \quad \text{(i.e. } (\mathscr{C}_3)_2\text{)}. \end{aligned}$$

To conclude, it suffices to remark that the inequality (i) above is nothing but $(\mathscr{C}_3)_1$ since a tedious but simple computation shows that

$$\alpha_1^2 - \alpha_0\alpha_2 = 4c_{11}c_{33}(c_{12}+c_{33})^2\Big[(c_{12}+c_{33})^2 - (c_{22}-c_{33})(c_{11}-c_{33})\Big]. \qquad \square$$

References

[1] S. Abarbanel, D. Gottlieb, J.S. Hesthaven, Well-posed perfectly matched layers for advective acoustics, J. Comput. Phys. 154 (2) (1999) 266–283.
[2] S. Abarbanel, D. Gottlieb, J.S. Hesthaven, Long time behavior of the perfectly matched layer equations in computational elactromagnetics, J. Sci. Comput. 17 (1–4) (2002) 405–422.
[3] B.A. Auld, in: Acoustic Fields and Elastic Waves in Solids, vols. I and II, Wiley, New York, 1973.
[4] E. Bécache, P.G. Petropoulos, S. Gedney, On the long-time behavior of unsplit perfectly matched layers, Technical Report 4538, INRIA, 2002, submitted.
[5] E. Bécache, A.-S. Bonnet-Ben Dhia, G. Legendre, Perfectly matched layers for the convected helmholtz equation, Rapport de Recherche, INRIA, 2002, accepted in SINUM.
[6] E. Bécache, P. Joly, On the analysis of Bérenger's perfectly matched layers for Maxwell equations, M2AN 36 (1) (2002) 87–120.
[7] E. Bécache, P. Joly, S. Fauqueux, Stability of perfectly matched layers, group velocities and anisotropic waves, Rapport de Recherche 4304, INRIA, 2001.
[8] E. Bécache, P. Joly, C. Tsogka, Fictitious domains, mixed finite elements and perfectly matched layers for 2D elastic wave propagation, J. Comput. Acoust. 9 (3) (2001) 1175–1203.
[9] E. Bécache, P. Joly, C. Tsogka, A new family of mixed finite elements for the linear elastodynamic problem, SIAM J. Numer. Anal. 39 (6) (2002) 2109–2132 (electronic).
[10] J.P. Bérenger, A perfectly matched layer for the absorption of electromagnetic waves, J. Comput. Phys. 114 (1994) 185–200.
[11] J.P. Bérenger, Three-dimensional perfectly matched layer for the absorption of electromagnetic waves, J. Comput. Phys. 127 (2) (1996) 363–379.
[12] J.P. Bérenger, Improved PML for the FDTD solution of wave–structure interaction problems, IEEE Trans. Antennas Propag. 45 (3) (1997) 466–473.
[13] W.C. Chew, W.H. Weedon, A 3D perfectly matched medium from modified Maxwell's equations with stretched coordinates, IEEE Microwave Opt. Technol. Lett. 7 (13) (1994) 599–604.
[14] G. Cohen, S. Fauqueux, Mixed finite elements with mass-lumping for the transient wave equation, J. Comput. Acoust. 8 (2000) 171–188.
[15] F. Collino, Perfectly matched absorbing layers for the paraxial equations, J. Comput. Phys. 131 (1) (1997) 164–180.
[16] F. Collino, P. Monk, Conditions et couches absorbantes pour les équations de Maxwell, in: G. Cohen, P. Joly (Eds.), Aspects récents en méthodes numériques pour les équations de Maxwell, Ecole des Ondes, Chapter 4, INRIA, Rocquencourt, 1998.
[17] F. Collino, C. Tsogka, Application of the pml absorbing layer model to the linear elastodynamic problem in anisotropic heterogeneous media, Geophysics 66 (1) (2001) 294–307.
[18] J. Diaz, P. Joly, Stabilized perfectly matched layers for advective acoustics, in: Proceedings of the 6th International Conference on Mathematical Aspects of Wave Propagation, Jyvaskyla (Finland), June 30th–July 4th, 2003.
[19] T. Fouquet, Personal communication.
[20] T. Hagstrom, I. Nazarov, Absorbing layers and radiation boundary conditions for jet flow simulations, in: Proceedings of the 8th AIAA/CEAS Aeroacoustics Conf., 2002.
[21] F. Hastings, J.B. Schneider, S.L. Broschat, Application of the perfectly matched layer (PML) absorbing boundary condition to elastic wave propagation, J. Acoust. Soc. Am. 100 (1996) 3061–3069.
[22] J.S. Hesthaven, On the analysis and construction of perfectly matched layers for the linearized Euler equations, J. Comput. Phys. 142 (1998) 129–147.
[23] R.L. Higdon, Initial-boundary value problems for linear hyperbolic systems, SIAM Rev. 28 (2) (1986).
[24] F.Q Hu, On absorbing boundary conditions for linearized euler equations by a perfectly matched layer, J. Comput. Phys. 129 (1996) 201–219.
[25] T. Kato, Perturbation Theory for Linear Operators, Springer, Berlin, 1980.
[26] H.-O. Kreiss, J. Lorenz, Initial-Boundary Value Problems and the Navier–Stokes Equations, in: Pure Appl. Math., vol. 136, Academic Press, Boston, USA, 1989.
[27] J. Métral, O. Vacus, Caractère bien posè du problème de Cauchy pour le système de Bérenger, C.R.A.S., I Math. (10) (1999) 847–852.

[28] P.G. Petropoulos, Reflectionless sponge layers as absorbing boundary condition for the numerical solution of Maxwell's equations in rectangular, cylindrical, and spherical coordinates, SIAM J. Appl. Math. 60 (3) (2000) 1037–1058.
[29] P.G. Petropoulos, L. Zhao, A.C. Cangellaris, A reflectionless sponge layer absorbing boundary condition for the solution of Maxwell's equations with high-order staggered finite difference schemes, J. Comput. Phys. 139 (1) (1998) 184–208.
[30] A.N. Rahmouni, Des modèles PML bien posés pour divers problèmes hyperboliques, Ph.D. Thesis, Universitè Paris Nord-Paris XIII, 2000.
[31] C.M. Rappaport, Perfectly matched absorbing conditions based on anisotropic lossy mapping of space, IEEE Microwave and Guided Wave Lett. 5 (3) (1995) 90–92.
[32] C.K.W. Tarn, L. Auriault, F. Cambuli, Perfectly matched layer as an absorbing boundary condition for the linearized Euler equations in open and ducted domains, J. Comput. Phys. 144 (1) (1998) 213–234.
[33] F.L. Teixeira, W.C. Chew, On causality and dynamic stability of perfectly matched layers for FDTD simulations, Microwave Opt. Technol. Lett. 17 (1998) 231–236.
[34] L.N. Trefethen, Group velocity in finite difference schemes, SIAM Rev. 24 (2) (1982).
[35] L.N. Trefethen, Group velocity interpretation of the stability theory of gustafsson, kreiss and sundström, J. Comput. Phys. 49 (2) (1983).
[36] L.N. Trefethen, Instability of difference models for hyperbolic initial boundary value problems, Commun. Pure Appl. Math. 37 (1984) 329–367.
[37] E. Turkel, A. Yefet, Absorbing PML boundary layers for wave-like equations, Appl. Numer. Math. 27 (4) (1998) 533–557.
[38] L. Zhao, A.C. Cangellaris, A general approach for the development of unsplit-field time-domain implementations of perfectly matched layers for FDTD grid truncation, IEEE Microwave and Guided Lett. 6 (5) (1996).
[39] L. Zhao, A.C. Cangellaris, GT PML: generalize theory of perfectly matched layers and its application to the reflectionless truncation of finite-difference time-domain grids, IEEE Trans. Microwave Theory Technol. 44 (1996) 2555–2563.